2.0 Literature Review

2. Literature Review

2.1 Introduction

This chapter focuses on the literature pertinent to injection molding pregenerated microcomposites and is separated into four sections. First, the area of injection molding in situ composites is discussed in section 2.2. This section clearly illustrates what disadvantages exist with in situ thermotropic liquid crystalline polymer (TLCP) composites, concluding with an evaluation of the problems with this method and how the pregenerated microcomposite process may solve them. Section 2.3 reviews injection molding of pregenerated microcomposites. The results of previous research are delineated, concluding with a summary of what questions still remain to be answered in this area. Section 2.4 covers fundamental concepts of injection molded fiber filled systems. As we are dealing with pregenerated TLCP fibrils which may behave in a fashion similar to glass systems, we want to know the factors which affect the properties of fiber reinforced composites. Furthermore, there may be differences in the processing behavior and mechanical properties of the pregenerated TLCP fibril systems relative to glass filled systems. In this section, the different forms of fiber reinforcement, rheology of suspensions, processing effects on fibers, and the mechanical properties of filled samples will be examined to understand these factors. Each area contrasts conventional fiber reinforcement with TLCP fibrils, emphasizing where differences exist. The final section will reiterate the objectives of the research and mention supplementary work needed to fulfill those objectives.

2.2 Injection Molded In Situ Composites

A broad introduction to TLCP reinforced thermoplastic composites was presented in Chapter 1. This section will provide a more detailed examination of injection molded in situ composites [1- 57]. The focus will be on two factors: 1) the shortcomings of in situ composites and 2) the effect of processing variables on mechanical properties. Developing this background will establish why other approaches to using TLCPs as reinforcement are needed and will serve as a point of comparison with pregenerated microcomposites.

2.2.1 Shortcomings of In Situ Composites

TLCPs used in the generation of in situ composites have been observed to fall short of fulfilling their reinforcing potential in two key respects. First, the transverse direction is usually not well reinforced, producing samples with mechanical anisotropy [39

- 41, 51 - 53]. Second, the experimental properties are lower than theoretical expectations, because not all of the TLCP is deformed into long fibrils with high molecular orientation [1, 3, 5, 6, 10 - 12]. Because these difficulties exist, an understanding of the causes must be achieved so potential solutions can be developed.

One cause of these problems are the flow kinematics which exist during the mold filling process. The best flow for orienting the TLCP phase is extensional [58- 63]. However, only the material at the leading edge of the advancing front is elongated by fountain flow kinematics. The melt in the center region following the advancing front is exposed to shear flow or a mixture of shear and extensional deformation, depending on mold geometry [64, 65].

One result of the complex mold filling flow kinematics is it produces a skin-core morphology in the composite. The melt at the advancing front becomes the skin of the composite because it is stretched and laid against the mold wall. This produces a surface layer which contains fibrils of high aspect ratio and molecular orientation. Meanwhile, the core is formed by the shear deformation which follows the advancing front. This flow is less effective in forming the TLCP into fibrils and may just leave spherical TLCP domains in the center of the sample if the viscosity of the matrix is lower than that of the TLCP [66].

A detailed description of in situ composite skin-core morphology was given by Silverstein et al. [17]. They examined blends of PET/Vectra A900 at loadings of 5, 25, 50, 75 and 95 wt% TLCP. A structural hierarchy was noted in these blends, with as many as six sublayers being discernible through the size, shape, and orientation of the TLCP domains (shown in Figure 2.1). This structural hierarchy was characterized by a gradient in structure consisting of a skin highly oriented in the flow direction and proceeding to a generally unoriented core, matching the observations of other researchers [1, 3, 5, 6, 10 - 12, 14].

The observation that in situ composites have a skin-core morphology helps to explain the existence of anisotropy and inefficient use of the TLCP as a reinforcing phase. Because the TLCP is oriented only the flow direction, the matrix is reinforced just in that direction. Therefore, it should be expected that these materials would possess anisotropic mechanical properties. The morphological analysis also demonstrates that not all of the TLCP is reinforcing the matrix. This is because some of the TLCP is not being formed into long fibrils with high molecular orientation. The absence of complete fibrillation of the TLCP domains suggests the reason for the composite not being stiffened as much as theoretically possible.

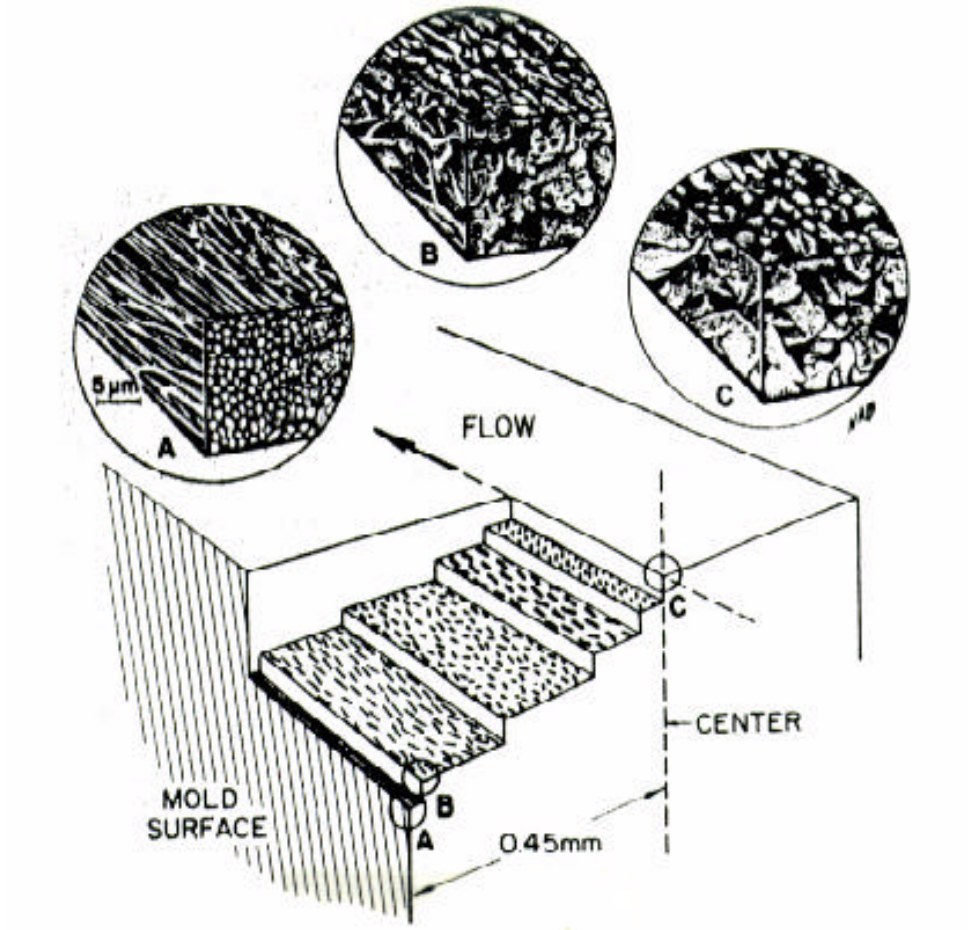

Figure 2.1: Structural Hierarchy of TLCP/Matrix Blends. As an injection molded sample is examined from the skin to the core, the morphology dramatically changes [17].

The second cause of the problems with in situ composites is the transfer of heat from the sample [39 - 41]. This is because the temperature must be high enough to allow fibrillation of the TLCP, yet cool enough so once the fibrils are formed they are quickly solidified upon cessation of flow. However, it is difficult to be at this temperature through the entire thickness of the specimen. This is because beneath the skin of the specimen, the polymer remains hot for a longer period of time, preventing the deformed TLCP phase from solidifying rapidly.

To illustrate that heat transfer in the formation of in situ composites is important, consider two plaques, 1.0 and 2.3 mm thick, respectively, which start with a temperature of 295°C and are in intimate thermal contact with a mold at 20°C. To reach a temperature of 200°C one-third of the distance into the plaque, it takes 0.25 seconds for the 1.0 mm thick sample and 1.4 seconds for the 2.3 mm thick sample [40]. Exposing the TLCP fibrils to this heat could allow molecular or morphological relaxation. This would reduce the reinforcing ability of the TLCP, producing a composite which would have mechanical properties lower than would be expected from theoretical calculations.

An additional consideration in the generation of in situ composites is the cooling characteristics of the TLCP phase. O'Donnell and Baird [40] demonstrated that the starting melt temperature of the TLCP affects the supercooling rheology of Vectra A950. Cooling curves were run at 295°C and 300°C and the complex viscosity was significantly changed. When cooled from 295°C, the dynamic viscosity was about a half an order of magnitude greater than when cooled from 300°C. This is important because the TLCP must be able to be stretched into high aspect ratio fibrils in order to maximize mechanical properties. To accomplish this, O'Donnell and Baird anticipated that for the TLCP phase to be highly deformable when processed from 295°C, it had to be kept hot by either rapidly filling the mold or by using high mold temperatures.

Rheological tests are also needed to reveal where the TLCP phase changes from liquid-like behavior ($G' < G''$) to solid-like behavior ($G' > G''$). This has been shown to be important for injection molding in situ composites because the maximum mechanical properties are obtained when the storage modulus (G') and loss modulus (G") are approximately equivalent [40 - 41]. For example, cooling curves on LC3000 revealed that $G' \approx G''$ when the starting melt temperature was 250°C. Meanwhile, when injection molding neat LC3000 into a 1.0 mm thick end-gated mold, the flexural modulus was 15.79 GPa when the melt was at 230°C, 17.46 GPa at a melt temperature of 250°C, and 15.78 GPa with the melt at 265°C. Therefore, the maximum mechanical properties were produced when following the condition that the storage and loss moduli should be approximately equal.

Summarizing, the problems of anisotropy and inefficient use of the TLCP as reinforcement need to be solved. It is realized that these difficulties are primarily due to 1)

the mold filling flow kinematics, 2) heat transfer within the mold, and 3) the cooling characteristics of the TLCP. Anisotropy is a result of the mold filling flow kinematics, with the TLCP being stretched only in the direction of flow. Meanwhile, inefficient use of the TLCP is a result of both the mold filling flow kinematics and heat transfer, with both of these causes primarily affecting the TLCP in the regions beneath the sample's skin. During the filling of film-gated plaque molds, extensional deformation is only imparted to the molten polymer at the advancing front. Therefore, it is unlikely that TLCP in the center of the sample is being elongated enough to realize all of its reinforcing potential. In addition, any oriented TLCP in the core of the specimen is going to be take longer to cool, allowing it to relax.

2.2.2 The Effect of Processing Variables on Mechanical Properties

In attempting to overcome these shortcomings, several areas have been investigated: 1) compatibilization, 2) ternary blending, 3) adding glass fibers to the matrix/TLCP blends, 4) modifying flow kinematics, 5) improving the dispersion of TLCP in the matrix through mixing, and 6) changing injection molding conditions. Each of these variables has shown the ability to affect mechanical properties. Therefore, it is necessary to demonstrate that although these variables can be used to improve composite mechanical properties by reducing anisotropy and/or increasing mechanical performance, alternative methods of processing will still be required to produce a composite with the desired mechanical properties.

2.2.2.1 Compatibilization

Compatibilization has been noted to have dramatic effects on morphology, with the TLCP being dispersed more effectively, creating smaller fibrils, making the composite surfaces smoother, and allowing less fiber pullout [18, 25, 34, 36, 42, 50, 51]. A more fibrillar structure has been observed with an increase in TLCP dispersion, thereby improving the ability of the TLCP to reinforce the matrix [42]. For example, O'Donnell and Baird [42] found that tensile bars of PP/Vectra A950 (70/30 wt%) had a tensile modulus of 4.2 GPa without compatibilizer, but improved to 4.8 GPa when 20 wt% maleic anhydride polypropylene (MAP) was added to the PP as a compatibilizer. It was also noted that when the in situ composite had 50 wt% MAP, the stiffness dropped to 3.6 GPa. Morphological examinations revealed that the TLCP domains were smaller than those in the other PP/Vectra A950 blends, leading O'Donnell and Baird to conclude that the addition of too much MAP reduced the interfacial surface tension to the point where fibril formation was hindered, reducing their aspect ratios.

Although the addition of compatibilizer created a finer morphology and increased the modulus, the highest stiffness is still well below the values predicted by composite theory. Due to the converging flow kinematics in the tensile bars, these materials should

follow the rule of mixtures for uniaxial reinforcement. For a PP/Vectra A950 (70/30 wt%) blend, complete orientation of the TLCP phase would produce a modulus of 15.3 GPa, over three times what was observed experimentally. Even for a random planar arrangement of TLCP fibrils, a modulus of 6.5 GPa should be reached. Therefore, the compatibilizer has improved the stiffness of the composite, but not enough to reach the maximum possible value.

Compatibilization has also been reported to improve the tensile strength of in situ composites because of improved adhesion between the two polymer phases [18, 25, 28, 29, 32, 34, 36, 39, 40, 42, 50, 51]. O'Donnell [39, 42] showed this by studying injection molded plaques of PP/Vectra B950 (70/30 wt%) with maleated polypropylene (MAP) content varying from 0 to 30 wt%. Using contact angle data, the work of adhesion for PP/Vectra B950 blends was 58.0 mN/m, while adding 10 wt% MAP to the PP increased the work of adhesion to 62.8 mN/m. This increase in adhesion was reflected in tensile properties of these in situ composites. The PP/Vectra B950 blend without MAP had a machine direction strength of 23.1 MPa and a strength of 11.8 MPa in the transverse direction. Meanwhile, the PP(MAP)/Vectra B950 (49/21/30 wt%) blend had strengths of 40.3 and 17.8 MPa in the machine and transverse directions, respectively. This was an increase of over 50% in both directions from the uncompatibilized composite values.

Not only have improvements in strength and modulus been reported, a reduction in anisotropy can also occur with the use of compatibilizers. Datta and Baird [51] demonstrated this by injection molding composites composed of PP/Vectra A950 (50/50 wt%) and PP/MAP/Vectra A950 (45/5/50 wt%), then comparing their tensile modulus. The PP/Vectra A950 plaques had a machine direction tensile modulus 4.523 GPa and a transverse direction modulus of 1.084 GPa, a property ratio of 4.17. Meanwhile, the samples containing MAP had a machine direction tensile modulus of 5.205 GPa and a transverse modulus of 1.567 GPa, a ratio of 3.32. It should also be noted that adding MAP improved the machine direction tensile strength from 26.43 MPa to 40.69 MPa.

However, even with reductions in anisotropy and increases in stiffness, the mechanical properties are not as high as theoretically possible. A random planar composite would have a modulus of 12.0 GPa if all of the Vectra A950 was being used to stiffen the PP/Vectra A950 (50/50 wt%) specimens. Therefore, neither the machine nor transverse direction properties are close to the expected values. For example, to reach the highest modulus of 5.205 GPa, experimentally it required 50 wt% Vectra A950, while composite theory predicts that only 20 wt% TLCP is necessary to have a planar isotropic modulus of 5.270 GPa. Therefore, although compatibilizers do significantly improve on the problems of anisotropy and incomplete utilization of the TLCP phase, further improvements are needed.

2.2.2.2 Ternary Blends

Ternary blending has been performed as a method of improving in situ composite mechanical properties [27, 43, 44, 45, 49]. For example, Kim and Hong [49] blended two matrix thermoplastics with one TLCP, examining what effect adding polysulfone (PSF) would have on the tensile strength of injection molded blends of polyphenylene sulfide (PPS) and Vectra B950. They found that adding PSF improved the strength of these blends, especially at low TLCP concentrations. For example, the PPS/Vectra B950/PSF blend with a composition ratio (CR) of 70/10/30 had a tensile strength of 70 MPa, while the PPS/Vectra B950 blend (CR = 100/10) had a strength of only 55 MPa. There were two reasons given for the improvement in strength: 1) PSF increased the blend viscosity, helping deform the TLCP domains and 2) the PSF reduces the free volume at the interface of the crystalline polymers in the blend, producing better adhesion.

Rather than blending a thermoplastic/wholly aromatic TLCP with a third thermoplastic, another approach has been attempted where the third polymer was a semiflexible TLCP. This was done with the belief that a semiflexible TLCP may improve mechanical properties by being compatible with both the wholly aromatic TLCP and the matrix polymer. Sun and coworkers [43 - 45] explored the potential of this idea by adding Rodlan, copolymers of poly(ethylene terephthalate) and 4-hydrobenzoic acid, as the third component in their ternary composites. They found that including Rodlan enhanced the degree of orientation of the wholly aromatic TLCP, resulting in improved mechanical properties. For instance, the Vectra A950/polycarbonate (PC) (30/70 wt%) blend had a tensile modulus of 1.9 GPa and a strength of 72 MPa, while the Vectra A950/Rodlan R5/PC (3/27/70 wt%) blend had the tensile modulus rise to 3.8 GPa and the strength increase to 125 MPa. The addition of a third component also changed the morphology, creating longer and finer TLCP fibrils. This suggests that Rodlan is successful in acting like a compatiblizer for both the matrix and TLCP.

Despite the fact that a rise in mechanical properties was noted by adding a third component, this increase was not enough to reach theoretical expectations. The tensile modulus of the Vectra A950/Rodlan R5/PC (3/27/70 wt%) blend was still well below theoretical predictions. For a random planar orientation, a stiffness of 7.4 GPa would be measured for this composite if all of the TLCP was being deformed into highly oriented TLCP fibrils. The experimental results are half of what composite theory predicts, indicating that although adding Rodlan R5 may improve mechanical properties, a significant amount of TLCP was not being oriented.

2.2.2.3 Addition of Glass Fibers

The influence of glass fibers on anisotropy was the subject of one investigation using PEI/HX1000 and PEI/HX4000 blends [35]. Three types of PEI, containing glass

fiber loadings of 0, 10, and 30 wt%, were mixed with TLCP pellets and injection molded to make in situ composites. The results showed that glass fiber has the potential to reduce mechanical anisotropy. For example, the 70/30 wt% blend of PEI/HX4000 had a machine direction flexural modulus of 7.00 GPa and a transverse modulus of 3.21 GPa, resulting in a property ratio of 2.18. Replacing the neat PEI with PEI filled with 30 wt% glass fiber reduced this ratio to 1.96, with the machine direction being 10.20 GPa and the transverse direction 5.20 GPa. This shows that, by adding fibers, anisotropy can be reduced without sacrificing machine direction properties.

Adding glass fibers to the in situ composites does not maximize the reinforcing potential of the TLCP phase, though. For instance, the machine direction modulus was 7.5 GPa for the PEI/HX1000 (70/30 wt%) composition and 11.1 GPa for the PEI/glass fiber/HX1000 composition of 49/21/30 wt%. This is close to the stiffness expected for a planar isotropic composite, with the theoretical modulus being 8.15 GPa when no glass was included and 11.4 GPa when the composite had 21 wt% glass fiber. However, the transverse direction properties did not approach these theoretical levels. The unfilled PEI/HX1000 plaque had a transverse direction modulus of 2.8 GPa, while the PEI/glass fiber/HX1000 (49/21/30 wt%) composite possessed a stiffness of just 5.0 GPa. Therefore, incorporating glass fibers into in situ composite blends does not produce composites with the desired mechanical performance.

Also, it should be noted that the addition of glass fibers creates some new problems. It increases the density of the blend, defeating one of the reasons for using TLCPs as a reinforcing phase. It was also noted that glass fiber worsens the processability of the blend [35]. Therefore, using glass fibers to reduce anisotropy is at best an imperfect solution to this problem.

2.2.2.4 Modifying Flow Kinematics

The influence of mold geometry on flow kinematics has been investigated by comparing injection molded plaques and tensile bars [34, 36, 51]. From this work, it has been shown that tensile bars have higher mechanical properties than the machine direction properties of film-gated injection molded plaques. For instance, in PP/Vectra B950 (80/20 wt%) blends, the tensile bars had a modulus of 2.876 GPa and a strength of 26.45 MPa [34]. Meanwhile, the plaques had just a modulus of 2.553 GPa and a strength of 24.04 MPa. The disparity is due to the converging flow produced in filling the dog bone shaped mold. This stretches the core of the sample in the machine direction, adding to the stiffness supplied by the highly oriented skin. In contrast, there is no extensional flow in the core of the plaques as they are being molded, leaving the skin to provide most of the reinforcement. Still, the uniaxial converging flow for a dog bone mold is not able to fully elongate all of the TLCP domains. This is shown by comparing the experimental modulus to that predicted by composite theory. Using the rule of mixtures composite theory and

assuming complete uniaxial reinforcement with the stiffest Vectra B950 fibrils, the 2.876 GPa measured for tensile bars is only 25% of the theoretically expected value of 11.77 GPa.

In an effort to reduce the mechanical anisotropy of in situ composites, Smartt and Baird [52, 53] evaluated the effect of using a center-gated mold. This is based on the idea that if the core can be stretched in the transverse direction, there exists the potential for reducing the anisotropy in these composites and fully utilizing all of the TLCP. The first published study compared the mechanical properties from samples produced with a film-gated rectangular mold to those from a center-gated mold [52]. The reason for using two molds is because the film-gated mold produces a linear flow front, so the core is not subjected to any extensional deformation. Meanwhile, a center-gated mold creates a spreading radial flow, stretching the core as the melt moves outward. The blends used were PET/Vectra B950 and PET/HX1000, at concentrations of 10, 20, and 30 wt% TLCP. From the transverse (or hoop) direction mechanical properties, it was concluded that not enough extensional flow was present to significantly deform the TLCP phase in the core region. This was shown by the transverse direction properties of the film-gated mold being the same as the properties of the center-gated mold, with both having a tensile moduli of about 2.5 GPa at loadings of 20 wt% HX1000 and Vectra B950. This is significantly below the theoretical planar isotropic values of 5.92 GPa and 7.16 GPa for 20 wt% loadings Vectra B950 and HX1000, respectively, and demonstrated that anisotropy was not reduced by increasing transverse direction modulus.

However, it should be noted that further work demonstrated reductions in anisotropy by both increasing hoop direction modulus and reducing the radial direction modulus [53]. This confirms other investigations showing that flow kinematics can affect mechanical properties of both neat TLCPs [67, 68] and matrix/TLCP blends [34, 36, 51]. However, further work needs to be done to prove if this is a viable method of reducing anisotropy. This would include: 1) using a small pinpoint gate to introduce the melt into the mold rather than a sprue bushing with an expanding gate and 2) varying processing conditions.

2.2.2.5 Mixing

Often the matrix/TLCP blends are compounded in an extruder directly before injection molding, but little data has demonstrated that the additional mixing improves mechanical properties [4, 32]. Isayev and Modic [4] examined the effect of mixing by generating two sets of end-gated disks composed of 90 wt% polycarbonate (PC) and 10 wt% LCP-2000, a form of Vectra A950. The first set of disks was injection molded at a barrel temperature of 310°C. Meanwhile, the second set of disks was produced using two processing steps; an extrusion step through six Koch static mixers, then injection molded at 310°C. Therefore, the only difference between the two sets of in situ composites is the

degree of mixing to which the two components have been subjected; in both cases the composite is formed during mold filling. They found that the addition of an extrusion blending step significantly improved mechanical properties in both the machine and transverse direction. The blend subjected to additional mixing had a machine direction modulus of 3.42 GPa and a transverse direction modulus of 2.26 GPa, versus the directly injection molded disks which had properties of 2.57 and 1.91 GPa, respectively. Still, it should be noted that if all of the TLCP had been oriented in a planar isotropic fashion, both the machine and transverse direction moduli would have been 3.53 GPa. This demonstrates that mixing may have increased the composite's stiffness, but not to the maximum level theoretically possible.

In other investigations, no improvement was achieved by mixing [7, 33, 36, 69]. Brinkmann and coworkers [69] investigated the relationship between viscosity and mixing using a novel approach, coupling one extruder into the barrel of a second. By doing this, they could effectively control the thermal history of the HBA/HNA based TLCP before introducing it into the PBT matrix. They found that the mixing process did affect the morphology of the extruded pellets, with the longest, most homogeneous pellets produced in the highest viscosity ratio of 10:1. However, after injection molding this difference was generally eliminated and most of the samples showed identical mechanical properties when compared to those which were not previously mixed. For example, the PBT/TLCP (90/10 wt%) in situ composites produced using the most homogeneously mixed pellets had a penetration energy of 2.5 Nm, the same as those made by directly dry blending and injection molding.

Baird et al. [33] also showed that mixing had no effect using a different approach. Starting with PEI/HX4000 blends ranging in composition from 70/30 to 30/70 wt%, two sets of test samples were made. The first set was simply a tumbled blend of pellets which were directly injection molded. Meanwhile, the second set was extruded and pelletized before it was injection molding, subjecting it to two mixing and plastication steps. The mechanical data indicated that no statistically significant improvement was achieved by the additional extrusion step. At 50/50 wt%, the one step process produced plaques with a tensile modulus of 15.4 GPa and a strength of 109 MPa while the samples from the two step process had a modulus of 14.5 GPa and a strength of 117 MPa. These results were within the standard deviation of the tests, so mixing had no appreciable effect on the final mechanical performance of these in situ composites.

2.2.2.6 Injection Molding Conditions

The factors of injection speed, mold temperature, and mold thickness were all examined in a comprehensive series of studies by O'Donnell [39 - 42]. Of these three variables, only injection speed and mold thickness were found to significantly influence

mechanical properties. Varying the mold temperature from 20°C to 70°C had no discernible effect on the mechanical properties of the composites.

The effect of mold thickness for matrix/TLCP blends was found to be complex because thinner molds do not always produce the maximum mechanical properties. Instead, an optimal thickness can exist. For example, O'Donnell [39, 41] injection molded plaques 1.0 mm, 1.5 mm, and 2.3 mm thick composed of PP/MAP/Vectra B950 (63/7/30 wt%). The mold was kept at 50°C and the injection speed was varied. Comparing machine direction results on plaques injection molded at a volumetric flow rate of about 14.5 cm^3, the 1.5 mm thick plaque had the highest flexural modulus (5.10 GPa) and strength (60.5 MPa). This contrasts sharply with the properties of samples from the other two molds. Plaques from the 1.0 mm mold had a modulus of 3.71 GPa and a strength of 54.2 MPa, while 2.3 mm thick plaques possessed values of just 4.61 GPa and 54.5 MPa. However, it should be noted that other blends did show the expected trend of a thinner mold producing samples with higher mechanical properties [39, 40, 41].

It was determined that rather than attempting to correlate mechanical properties to mold thickness, they should be compared to the Graetz number [39, 41]. The Graetz number is a dimensionless group which indicates the magnitude of the heat convected in the down channel direction to the heat conducted in the transverse direction. Mathematically, it is formulated as:

$$\text{Equation 2.1:} \quad N_{GR} = \frac{U \cdot H^2}{\alpha \cdot L}$$

where U is the average velocity, H equals half the mold thickness, α is the thermal diffusivity, and L represents the mold length. It was found for each plaque thickness, the flexural modulus began to drop dramatically for Graetz numbers lower than 10. At these smaller Graetz numbers, it was speculated that the Vectra B950 begins to solidify, making the TLCP more difficult to deform into fibrils at the given velocity. Therefore, it is believed that this dimensionless group is useful in relating TLCP solidification and deformation to the observed mechanical properties.

However, even when processing at the optimum Graetz number for maximizing in situ composite properties, the theoretical moduli were not reached. The highest machine direction tensile modulus for the PP/MAP/Vectra B950 (63/7/30 wt%) blends was 4.74 GPa, using a 1.5 mm thick mold and an injection time of 2.7 seconds. The processing conditions for this material correspond to a Graetz number of 9, right around the critical Graetz number of 10 found to be necessary to attain the highest flexural properties. For this in situ composite, a random planar sample with 100% of the reinforcing potential of the TLCP would have a tensile modulus of 7.33 GPa. This figure is based on all of the TLCP being formed into highly molecularly oriented fibrils with aspect ratios over 100.

Therefore, the best machine direction stiffness was only 65% of the theoretically predicted isotropic value.

The influence of injection speed on mechanical properties is generally that faster injection speeds produce better machine direction flexural properties, but also greater anisotropy [39 - 41]. This was demonstrated in a blend of PP/MAP/Vectra B950 (63/7/30 wt%) [39, 41]. 1.5 mm thick plaques showed the highest mechanical properties when injected at the fastest time of one second. The machine direction flexural modulus and strength at this injection time were 5.10 GPa and 60.5 MPa, respectively, while the transverse direction modulus and strength were 1.80 GPa and 35.1 MPa. Raising the injection time to 10.7 seconds produced plaques with a machine direction modulus of 3.21 GPa and a strength of 52.1 MPa, an appreciable decline. Transverse direction properties were not measured for this injection time, but for injection times up to 4.4 seconds, the transverse direction moduli and strengths stayed around the 1.80 GPa and 35.1 MPa values measured for the fastest injection time. Therefore, faster injection speeds favorably improve machine direction properties, but have no influence on the reinforcement for the transverse direction.

O'Donnell's tensile test results had the same trends as the flexural data, with a machine direction tensile modulus of 4.18 GPa for the fastest time and just 2.85 GPa for the slowest injection time. It should be noted though, that if all of the TLCP molecules were completely oriented, formed into high aspect ratio fibrils, and distributed in the matrix in a random planar fashion, the stiffness would theoretically be 7.33 GPa, significantly greater than any of the experimental data. Therefore, increasing the injection speed does not correct the problems of anisotropy and incomplete use of the TLCP as reinforcement.

To summarize, the findings with in situ injection molded composites show that although TLCPs are able to reinforce thermoplastics, two critical problems exist. These problems are anisotropy and incomplete utilization of the TLCP's reinforcing potential. Neither problem has been satisfactorily solved using conventional injection molding approaches. Therefore, there is a need for some innovative processing schemes in attempting to overcome these limitations.

2.3 Injection Molded Pregenerated Microcomposites

One processing method which has the potential to eliminate the problems encountered in injection molding of in situ TLCP composites is the pregenerated microcomposite processing scheme [70]. This scheme relies on producing pellets containing oriented TLCP fibrils in one step and using a second step to form the desired product. The pellets are made by spinning blends of the TLCP with the desired matrix and

chopping the strands. Then they can then be injection molded below the melting point of the TLCP, but above that of the matrix [52, 70 - 78].

Producing pregenerated microcomposites by injection molding has been investigated because of the need to utilize the full reinforcing potential of the TLCP while reducing the anisotropy characteristic of in situ composites. This processing technique also has the benefits of creating a light weight composite using a process with fast cycle times. It provides a process analogous with glass-fiber filled polymer injection molding, but with several potential advantages. The composite will be lighter than a glass-filled sample because of the lower density of TLCPs. The TLCP fibrils are often 1μm or less in diameter, versus the 10-15 μm typically observed for glass fiber. Also, due to the spinning step necessary to generate the TLCP reinforcement, no compounding step is required to mix the matrix with the reinforcement.

The influence of processing temperature on the mechanical properties of injection molded samples has been examined in several studies [70 - 73, 77, 78]. Sabol et al. [77, 78] used PP(10 wt% MAP)/Vectra B950 (76/24 wt%) and changed the temperature of the third zone on the injection molder in 10°C increments, proceeding from a low temperature of 250°C to a high of 300°C. This is a processing range which crosses the 280°C melting point of Vectra B950, so it is comparing pregenerated to in situ reinforcement. He found the transverse direction tensile modulus stayed approximately constant at 1.75 GPa, while the machine direction modulus increased with higher temperatures. At 250°C, the modulus was 2.4 GPa, while at 290 and 300°C it rose to 3.75 GPa. This demonstrated that although the pregenerated microcomposites had more isotropic properties, this was due to lowering of machine direction reinforcement. The reason attributed for little property improvement was deformation and breaking of TLCP fibrils. This was shown by optical micrographs of the composites, with distorted fibrils being clearly discernible. As delineated in Chapter 1, Heino and coworkers [73] observed similar phenomena using a blend of PP/Vectra A950 (80/20 wt%). To avoid this problem, using a TLCP with a higher glass transition temperature or melting point was recommended [77].

As with the studies of pregenerated microcomposite sheets [70, 71] and blow molded bottles [70, 76], the effect of fiber draw ratio on the mechanical properties of pregenerated microcomposite injection molded plaques has been investigated [70, 72, 73]. Handlos [70, 72] examined the relationship between draw ratio and mechanical properties using blends of PP/Vectra A950 and PP/HX6000. The fibers of PP/Vectra A950 (60/40 wt%) had draw ratios of: 1) 4.7, 2) 20, and 3) 30, and the draw ratios of the PP/HX6000 fibers were: 1) 4, 2) 13.5, and 3) 25. These fibers were chopped into pellets, dry blended with more PP to bring the TLCP concentration down to 30 wt%, and injection molded at 190°C. From the mechanical properties of these composites, it was shown that increasing the draw ratio improved tensile strength and modulus. For example, the PP/HX6000

(70/30 wt%) pregenerated microcomposites had a machine direction tensile modulus of 3.20 GPa and a strength of 35.0 MPa when strands having a draw ratio of 4 were used. Meanwhile, strands with a draw ratio of 25 were injection molded to produce plaques with a modulus of 3.98 GPa and a strength of 38.4 MPa. However, it is still not known how high the mechanical properties would be if strands with draw ratios over 50 were the starting reinforcement.

Handlos [70] examined the anisotropy between pregenerated microcomposites versus glass-filled PP and found that they both showed about the same degree of anisotropy when injected into a film-gated plaque mold. For PP/glass (80/20 wt%), the ratio of machine direction to transverse direction modulus was 1.31. The two pregenerated microcomposites, PP/Vectra A950 and PP/HX6000, had ratios of 1.06 and 1.32. This appears to demonstrate that the TLCP fibrils and glass fibers have similar orientation distribution functions in the plaque, so a mold which produces an isotropic specimen using glass-fiber reinforcement should also do so for a pregenerated microcomposite.

The best mechanical properties obtained by this process were with PP(10 wt% MAP)/HX6000 blends. For a 30 wt% TLCP, the machine direction modulus was 3.98 GPa and its strength was 38.4 MPa. Meanwhile, the transverse direction had a modulus of 2.91 GPa and a strength of 19.9 MPa. Neat PP has a modulus of 1 GPa and a strength of 25.6 MPa, so although this does stiffen the PP matrix, the improvement of strength is negligible. This is despite the fact the polypropylene used contained 10 wt% maleated polypropylene to help interfacial bonding.

However, predicting composite stiffness from TLCP fiber moduli establishes that higher tensile moduli are possible. For the PP(10 wt% MAP)/HX6000 (70/30) composite, using the rule of mixtures composite theory, a planar isotropic modulus of 5.20 GPa is calculated if each HX6000 fibril has an aspect ratio over 100 and a modulus of 43 GPa. This is 30% greater than the experimental machine direction modulus and 79% greater than the transverse direction modulus. Two possible reasons for this discrepancy are 1) molecular relaxation due to the TLCP becoming too hot and 2) loss of aspect ratio due to the shear stresses in the injection molding step [70, 71, 77, 78].

In summary, the pregenerated TLCP fibrils do provide reinforcement to the matrix and do reduce mechanical anisotropy. On the other hand, the degree of reinforcement is only around 50% of that theoretically predicted. Therefore, some key questions remain to be answered:

1) It is still not known if this technique can be applied to blends containing matrices besides polypropylene. Polypropylene has a distinct advantage over some other commodity resins in it has a broad processing temperature window. It is necessary to

prove that other resins which have tighter processing constraints can also be reinforced in this manner.
2) The precise cause of property loss is still unclear. Although agglomeration has been observed in these systems, a more quantitative analysis has not been undertaken. Also, effects like loss of aspect ratio, fibril twisting, and thermal relaxation may contribute to property loss. These could significantly contribute to the negative deviation from the rule of mixtures composite theory which has been noted.
3) Finally, to date no results have been reported for pregenerated microcomposites in which the starting strands had the optimum mechanical properties.

2.4 Fiber-Reinforced Polymers: Fundamental Concepts

2.4.1 Fiber Reinforcement of Thermoplastics

The focus of this work is to use pregenerated TLCP fibrils which act like fiber reinforcement to improve mechanical properties. Toward that goal, it is necessary to state the drawbacks which are associated with this reinforcement and how the pregenerated microcomposite process has the potential to surmount some of these difficulties. The following paragraphs will do this using a two-tiered approach. First, a general listing of problems associated with processing fibers will be delineated, followed with suggestions on how the pregenerated microcomposite process can solve or avoid them. Second, the three major types of fiber reinforcement (glass, carbon, and aramid) will be introduced to compare and contrast their mechanical properties, fiber diameters, and costs.

Short glass fiber reinforcement has been noted to have several drawbacks. These include:

1) Requiring a higher processing temperature [7, 79, 80]
2) Having a higher viscosity than the neat thermoplastic, especially at low shear rates [7, 79, 80, 81, 82]
3) Altered flow characteristics when compared to the neat resin [79, 83, 119]
4) Needing higher injection pressures [79, 80]
5) Increased equipment wear due to interactions between the fiber and processing machinery [7, 80, 84, 85]
6) Production of anisotropic parts, both in terms of fiber orientation and stress distribution [79, 80, 83, 119]
7) Poorer surface finish due to surface waviness, sink marks, and a loss of high gloss finish [80, 119]
8) Development of weld lines [83, 86, 119]

9) Loss of aspect ratio during compounding and injection molding [84, 89]
10) Higher weight due to the density of glass

The pregenerated microcomposite process has the potential to address several of these problems. TLCP fibrils are often an order of magnitude smaller in diameter than glass fibers. Therefore, the surface finish problems could be less severe with these materials. Smaller fibers should also allow thinner molds to be used, because the fiber orientation will not be influenced as much by fiber-mold wall interactions. The TLCP reinforcement should more readily pass thorough the barrel, screw tip, nozzle exit, and mold gates of the injection molder, resulting in less wear on processing equipment. With TLCP densities nearly half that of glass, any TLCP based composites will be significantly lighter than their glass-based analogs.

However, to realize these potential advantages, the TLCP-based composites must have mechanical properties competitive to other forms of thermoplastic reinforcement. The three major forms of fiber reinforcement in injection molded articles are glass, carbon, and aramid (Kevlar®). Neat fiber characteristics are provided on Table 2.1. Each has specific advantages and disadvantages which need to be discussed to provide a comparison to TLCP fibers.

Glass based systems have the chief advantage of producing reinforcement at low material cost. Glass fiber costs around $1.65/kg [87]; this is over an order of magnitude cheaper than carbon, aramid, or TLCP fiber and translates directly into less expensive composites. For example, using the average costs cited on Table 2.1 and a polycarbonate (PC) price of $5.30/kg [96], 1 kg of 20 wt% glass fiber-filled PC has a material cost of $4.57 while 1 kg of 20 wt% carbon fiber-filled PC is $13.44. At this loading, a glass-filled polycarbonate sample has a tensile strength of 61.4 MPa and a modulus of 3.9 GPa while using carbon fiber produces a strength of 69.0 MPa and a stiffness of 8.6 GPa [215]. So, although the graphite yields better mechanical properties, that benefit is often offset by its high cost.

Despite the advantage of low cost, glass does possess some drawbacks. Its density is very high relative to the other forms of reinforcement, making glass reinforced composites heavy. This increased density makes glass' specific tensile modulus and strength lower than other forms of reinforcement (see Table 2.1). So, for applications where light weight is essential, glass fiber is a poor choice as a reinforcing material.

The chief asset carbon fiber based systems have are superior mechanical properties [88, 113]. This is well demonstrated by comparing short glass reinforcement with short carbon reinforcement. At 30 wt% fiber in polyamide 6,6 (PA 6,6, nylon 6,6),

Table 2.1: Neat Fiber Reinforcement Characteristics.

	Glass Fiber [89 - 91, 87]	Carbon Fiber [80, 92- 95, 114]	Aramid Fiber [116, 216]	TLCP Fiber [77 , 96 - 112]	Annealed TLCP Fiber (Vectra Series) [111]
Range of Cost/unit weight ($/kg)	1.65	22 to 2200	22 to 220	26 to 48	26 to 48
Average Unit Cost ($/kg)	1.65	46	33	37	37
Tensile Modulus (GPa)	69 to 83	207 to 637 (around 230 is typical)	128	40 to 100	40 to 100
Specific Tensile Modulus ($GPa \cdot cm^3/g$)	28 to 33	109 to 302 (around 130 is typical)	88.9	31 to 77	31 to 77
Tensile Strength (GPa)	1.72 to 2.07	2.24 to 2.65	3.79	0.5 to 1.0	0.5 to 2.0
Specific Tensile Strength ($GPa \cdot cm^3/g$)	0.69 to 0.83	1.17 to 1.30	2.63	0.7	1.4
Density (g/cm^3)	2.52 to 2.61	1.73 to 2.11	1.44	1.2 to 1.4	1.2 to 1.4
Fiber Diameter (μm)	0.5 to 14	7 to 10	12	Less than 1 to greater than 10	Less than 1 to greater than 10
Typical Diameter	10 to 13	7	12	2	2

short glass composites have a tensile strength of 186 MPa and a modulus of 9.65 GPa. Carbon fiber composites of PA 6,6 possess much higher tensile properties, with a strength of 241 MPa and a modulus of 20.7 GPa [113]. In addition to the better mechanical characteristics, the carbon based composite has a specific gravity of 1.28 while the glass fiber filled system is at 1.37. This shows that carbon fiber reinforcement produces a lighter, stronger, and stiffer composite than glass fiber [113].

However, carbon fiber has only replaced glass reinforcement in specific applications because of its substantial limitations. One difficulty is composites based on short carbon fiber have lower impact properties than glass fiber [80]. Notched Izod impact strength of 30 wt% short carbon fiber filled PA 6,6 is 80 J/m, while the same loading of glass reinforcement is significantly greater, at 107 J/m [113]. Also, typical carbon fiber is priced between $26/kg to $66/kg, significantly greater than glass fiber [80, 114, 115]. Therefore, for applications which need greater impact strength or low cost, carbon fiber is not an acceptable alternative form of reinforcement.

Aramid (poly(1,4-phenylene terephthalamide), Kevlar) based systems do not have the high mechanical properties that glass filled and carbon filled suspensions possess. For instance, with a long aramid fiber-filled polyamide 6,6 (nylon 6,6) composite (40 wt% reinforcement) the tensile strength is 117 MPa and the modulus is 8.27 GPa [113]. This is significantly lower than long glass fiber-filled PA 6,6, which at a loading of 30 wt% has a tensile strength of 196 MPa and a modulus of 10.0 GPa, and long carbon fiber-filled PA 6,6, which at the same 30 wt% loading has a strength of 248 MPa and a modulus of 25.5 GPa. Aramid fiber is also expensive, with an average price of about $33/kg [80, 116]. The low mechanical properties and high cost have made its use very limited.

However, aramid fiber does possess some unique advantages which allow it to be competitive in niche markets. One advantage of aramid fiber is it is more flexible than either carbon or glass fibers, so long aspect ratios are retained. This produces a composite which contains highly curled and entangled fibers, making the parts have more isotropic orientation [113, 171, 172]. They have also been noted to provide a substantial increase in wear resistance [88, 113, 117] and very good impact properties [80]. Its low density of around 1.44 g/cm^3 is another useful characteristic of Kevlar fiber. This is about 40% lower than glass and 20% less than commonly used carbon fibers [116]. These qualities have insured that specific markets will use Kevlar as the reinforcing phase.

It is clear that a combination of high mechanical properties, low density, and low cost is not available with these three forms of reinforcement. Therefore, TLCP composites either have to succeed in offering this combination of characteristics or come closer to this goal than the other three fibers. This potential does exist, for several reasons:

1. TLCPs have a density around 1.2 to 1.4 g/cm^3 which matches or is lower than any of the other forms of reinforcement.
2. TLCPs have specific moduli and strengths which match or exceed glass fiber. For annealed TLCPs, the specific tensile strength can exceed what is found for graphite.
3. TLCP fibrils are smaller in diameter than the other commonly used forms of reinforcement. This means the length of reinforcement does not have to be as great to receive the complete reinforcing potential of the TLCP fibril.
4. The spinning process fully wets the TLCP fibrils, which avoids the problematic compounding step encountered with the other forms of injection molded reinforcement [94, 115] and does not require the high pressure compression molding step needed to wet glass and carbon fiber woven prepregs [112, 118].
5. The long TLCP fibrils mean fewer fibril ends. This should produce smoother surface finishes, higher moduli, and greater strength, as is found for long-fiber reinforcement [113, 172].

These reasons demonstrate that a need for effective, light weight reinforcement does exist and the pregenerated microcomposite processing technique possesses attributes which may satisfy this need.

2.4.2 Rheology

Entraining solid particulates in a viscous polymer melt has definitive effects on how the material responds to deformation. This must be understood in order to properly process the polymer and attain the highest mechanical properties. Interest has been in response to both a better understanding of fluid flow and to aid the processing engineer in production. This can be divided into two major portions: 1) suspension theories and model equations and 2) experimental observations. The suspension theories will be developed from dilute Newtonian fluids to concentrated non-Newtonian melts. As this is done, the factors which cause the fiber-filled liquid to exhibit non-Newtonian behavior will be mentioned. The second portion will delineate the experimental observations found with filled polymer melts, concentrating on issues with solid fibers but mentioning other solids where needed.

2.4.2.1 Suspension Theories and Model Equations

The simplest suspension theories use small quantities of solids in a Newtonian fluid to predict viscosity. If the fluid is dilute enough, the particles behave as if they were alone in an infinite matrix and there are no fiber-fiber interactions. This criterion is satisfied if $(d/L)^2 < c$, where d is the fiber diameter, L is the fiber length, and c is the concentration of fibers in the suspending fluid [119]. The equations which predict the viscosities of these dilute suspensions can be summarized as follows [120]:

Equation 2.2: $\eta = \eta_f [1 + \alpha_0 \phi]$

where η is the suspension viscosity, η_f is the viscosity of the suspending fluid, ϕ is the volume fraction of the filler, α_0 is a dimensionless factor determined by the shape, dimensions, and orientations of the suspended particles. For rigid spheres, α_0 equals 2.5 and the equation becomes Einstein's formulation [121]:

Equation 2.3: $\eta = \eta_f [1 + 2.5\phi]$

Because fibers are poorly modeled as spheres, this equation is not effective for dilute fiber-filled systems. For those systems, a few other expressions for α_0 have been determined to be more accurate [122, 123]:

Expression 1: $$\alpha_0 = \left[\frac{1.15 \frac{L}{d}}{\pi \ln\left(2\frac{L}{d}\right)} \right]$$

Expression 2: $$\alpha_0 = \left[\frac{2\frac{L}{d}}{3\pi \ln\left(2\frac{L}{d} - 1.8\right)} \right]$$

These are based on the assumption that the initial fiber distribution is random.

However, these simple suspension theories are inadequate for semiconcentrated and concentrated systems because they do not account for several factors which can influence rheological behavior [120]. Non-hydrodynamic forces such as Brownian and van der Waals forces can affect the rheology when the particle size is under 1 μm. When particles are 10 μm or larger, the hydrodynamic interactions can cause a change in velocity distribution in the vicinity of other fibers. Fiber-fiber collisions may also influence suspension viscosity by creating anisotropic structures in the fluid.

These factors usually change the rheological behavior enough to transform most Newtonian fluids into non-Newtonian fluids. Examples of this include displaying nonzero first normal stress differences [124, 125] and, for aspect ratios over 40, showing shear thinning behavior and entrance pressure drops. Time-dependent viscosity has also been observed, because of the strain-dependent structure present in the fluid [120].

Because the simple suspension theories are not adequate for representing the viscosity of Newtonian fluids with semiconcentrated and concentrated loadings of solids, other empirical or semi-empirical formulas have been proposed [126]. One which has been successful in capturing the shear dependence of viscosity is the Cross equation [127]:

Equation 2.4: $$\left[\frac{\eta - \eta_\infty}{\eta_0 - \eta_\infty}\right] = \left[1 + (\lambda\dot{\gamma})^a\right]^{-1}$$

This closely resembles the Carreau-Yasuda empirical equation, with (n-1)/a = -1 [128]:

Equation 2.5: $$\left[\frac{\eta - \eta_\infty}{\eta_0 - \eta_\infty}\right] = \left[1 + (\lambda\dot{\gamma})^a\right]^{(n-1)/a}$$

Note that for both of these equations η is the fluid viscosity, η_o is the zero shear viscosity, η_∞ is the infinite shear viscosity, λ is a time constant, and $\dot{\gamma}$ is the shear rate. At low shear rates, the zero shear viscosity is produced, while high shear rates model the power law behavior which is typical for these systems.

The formulas postulated for fiber-filled Newtonian fluids are useful for predicting suspension viscosity, but filled-polymer melts require models which incorporate the inherent non-Newtonian nature of the neat fluid. Keentock [129] attempted this by using a Hershel-Bulkley model to predict the viscosity:

Equation 2.6: $$\eta = \tau_y(\dot{\gamma})^{-1} + k_C(\dot{\gamma})^{(n-1)}$$

where τ_y is the yield stress, κ_c is the consistency index, n is the power-law index, and $\dot{\gamma}$ is the shear rate. This incorporates the yield stress observed for heavily filled suspensions, but can not model filled systems which show a zero shear viscosity. There is no correlation made between aspect ratio and viscosity in this equation, which is known to affect how suspensions respond to force. Also, it uses a power-law description of the matrix viscosity, which is not always accurate.

To overcome the shortcomings of the Hershel-Buckley model, a more general empiricism was proposed by Poslinski and coworkers [130] (hereafter called the Poslinski model):

Equation 2.7: $$\eta = \tau_y(\dot{\gamma})^{-1} + \eta^0\left[1 + (\lambda_C\dot{\gamma})^2\right]^{(n-1)/2}$$

where:

$$\eta^0 = \eta_m^0\left[1 - \left(\frac{\phi}{\phi_m}\right)\right]^{-2}$$

and

$$l\ {}^{0}_{c} = l\ {}^{0}_{m}\left[1-\left(\frac{f}{f_m}\right)\right]^{-2}$$

η^0 is the suspension zero shear viscosity, $\eta_m{}^0$ is the neat matrix zero shear viscosity, $\lambda_i{}^0$ is the time constant, ϕ_m is the maximum packing parameter, and ϕ is the volume fraction of solids. Note i=c for the composite melt and i=m for neat matrix values. The workers found that this equation could predict *a priori* the suspension viscosity as a function of matrix rheology, volume fraction of particulates, and shear rate. This indicates that coupling the Hershel-Buckley equation with a Carreau equation shear dependence can model the viscosity behavior for the entire range of filler concentrations (illustrated in Figure 2.2).

In addition to the equations for shear viscosity, some work has been performed for extensional viscosity. Batchelor [131, 132] derived the following expression for dilute fiber-filled suspensions in a Newtonian fluid:

$$\text{Equation 2.8:}\quad h_e = \frac{2a^2 f h_{ef}}{9\ln a}\left[1+O(1/\ln a)\right] + h_e$$

where η_e is the extensional viscosity of the suspension, η_{ef} equals the extensional viscosity of the neat fluid, α is the aspect ratio of the fibers, and ϕ represents the volume fraction of fiber in the fluid. Meanwhile, for non-dilute concentrations of fiber, Batchelor [132] obtained this expression:

$$\text{Equation 2.9:}\quad h_e = 3h_{ef} + \frac{4}{3}h_{ef}\frac{(a)^2}{\ln(p/f)}$$

He stated that for this equation to be valid, two conditions must be met: 1) $\phi^{0.5}<<1$ and 2) $\phi^{0.5}\cdot(\alpha/2)>>1$. Experimental work by Mewis and Metzner [133] found that Equation 2.8 agreed well with dilute suspension in Newtonian fluids. However, very little experimental work has been performed to confirm either of Batchelor's equations when the neat fluid is nonNewtonian or viscoelastic, so their applicability toward fiber-filled polymer melts is an area warranting further research.

This synopsis on empiricisms for suspension viscosity is useful for pregenerated microcomposite melts because the TLCP fibrils should behave similarly to other fibers. Therefore, the Poslinski model should accurately predict the viscosity of these concentrated suspensions. Also, if pregenerated microcomposite melts show a viscosity dependence on processing and thermal history, these empiricisms may offer some insight

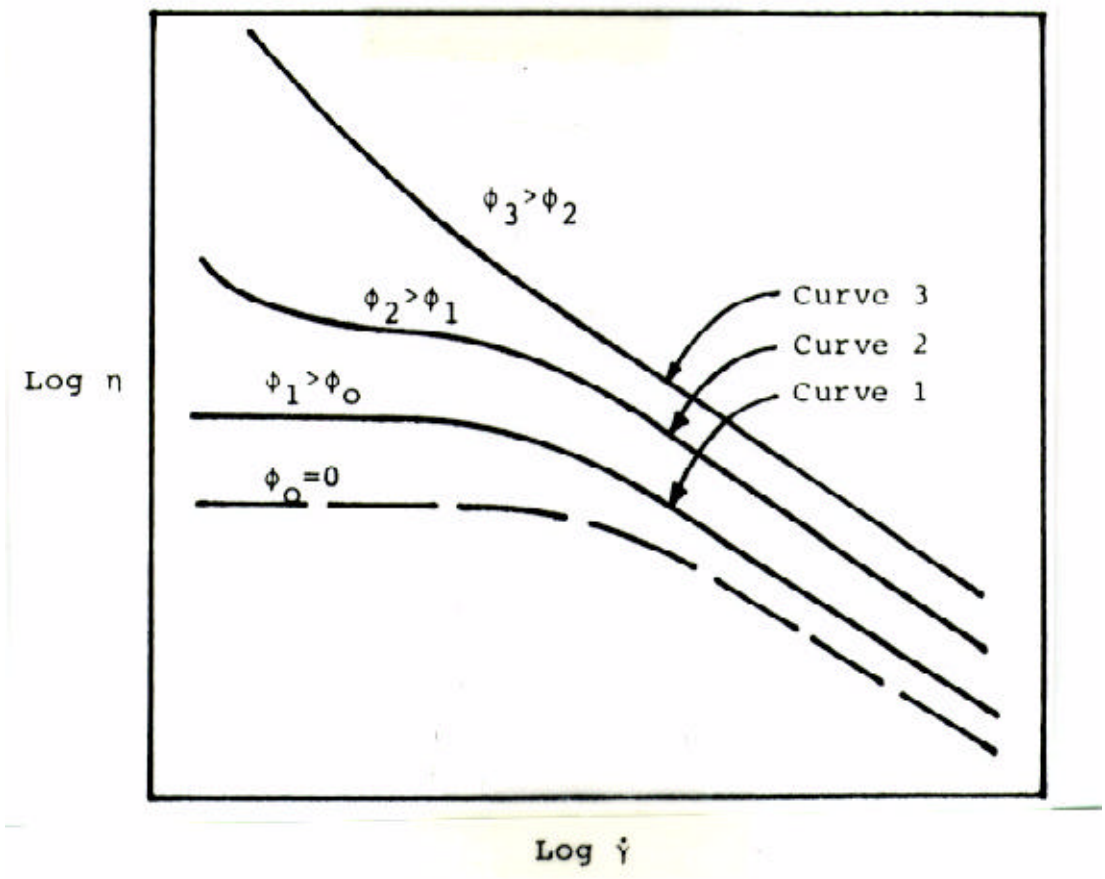

Figure 2.2: The Range of Viscosity Behavior the Poslinski Model Predicts. As the loading level of glass fibers increases, the zero shear viscosity plateau disappears [130]. Curve 1 shows low concentrations of solids (up to 10 vol%), curve 2 an intermediate range (around 20 vol%), and curve 3 a high concentration (30 vol% and greater), with ϕ_i being the volume fraction of the solids.

on possible causes. For example, shifts in viscosity may be attributed to changes in the shape of the reinforcement, which is encompassed in the Poslinski model's maximum packing parameter.

2.4.2.2 Experimental Observations

Filled polymer melts have been tested to determine how fibers affect steady shear and transient rheological behavior. Steady shear tests have been performed, with the viscosity being influenced by shear rate, fiber aspect ratio, fiber concentration, and the diameter of the filler. Transient tests on these concentrated suspensions have exhibited shear stress and first normal stress overshoots. Surface treatment has also shown to modify the rheology of filled polymer melts, so its influence will be mentioned.

The viscosity of concentrated fiber filled melts often does not exhibit a zero shear viscosity (η_0) , but rather increases with decreasing shear rate [120, 126, 134, 135]. This suggests the presence of a yield stress [135, 136]. For example, Laun [135] mixed low density polyethylene (LDPE) with glass fibers having an aspect ratio of 25 until it contained 30 wt% reinforcement. This suspension did not show a zero shear viscosity at 0.1/sec, but instead rose to nearly 10^7 Pa·sec at a shear rate of 10^{-4}/sec. This is three orders of magnitude greater than the value for neat LDPE. The high viscosity at low shear rates is due to the structure present in the melt [135, 137]. At low shear rates, the interaction between the fibers offsets the force attempting to align the fibers, creating substantial resistance to deformation. Increasing the shear rate overcomes the interactions, disrupting the structure formed by orienting the fibers with the flow.

However, not all fiber filled melts show a yield stress; low fiber concentrations often merely shift the zero shear viscosity plateau to low shear rates [126, 130]. Mutel [126] demonstrated this with blends of polypropylene (PP) and glass fibers. At loadings of 20 and 30 wt%, the viscosity increases with decreasing shear rate. Meanwhile, concentrations of just 5 wt% fiber shifted the highest shear rate with a zero shear viscosity to around 0.02/sec, versus 0.06/sec for neat PP.

Aspect ratio also affects whether a yield stress is observed. Laun [135] examined the effect of aspect ratio using polyamide 6 (PA6, nylon 6) as the matrix. When a melt containing 30 wt% glass was used, aspect ratios of 10 and lower generated a Newtonian plateau at low shear rates (around 10/sec). Meanwhile, glass with an aspect ratio of 25 had the suspension viscosity continually rise to the 10^{-2}/sec shear rate limit of the equipment. At this low of a shear rate, the viscosity was around $7 \cdot 10^3$ Pa·sec for the long fiber-filled melt, while the zero shear viscosity of the short fiber-filled PA6 was only around $4 \cdot 10^2$ Pa·sec.

Adding more fiber increases the suspension viscosity, but this rise is a function of shear rate [120, 126, 135]. The change in viscosity is well illustrated by comparing neat low density polyethylene (LDPE) to LDPE with 30 wt% fiber [135] (shown in Figure 2.3). At 1/sec, the filled LDPE has a viscosity of 1000 Pa·sec versus 500 Pa·sec for the neat material. Although this difference is substantial, it pales when comparing the two melts at $1 \cdot 10^{-3}$/sec, where the fiber-filled polymer is two hundred and fifty times more viscous. This shows that at low shear rates, structural features significantly increase the resistance to deformation, but at high shear rates these effects are eliminated and the viscosity is only moderately greater.

Higher viscosities are also produced by using smaller diameter fibers. Laun [135] examined the viscosity of 30 wt% glass filled PA 6, with the fiber aspect ratio being 25. Two different glass fibers were used, one with a diameter of 10 μm and the second with a diameter of 13.5 μm. For the range of shear rates tested (0.1/sec to 100/sec), the melt with 10 μm fibers was more viscous. The increased viscosity was attributed to a higher number density of glass fibers at the same weight concentration, meaning there are more fibers per unit volume with the smaller diameter fibers. This produces more fiber-fiber interactions, which makes the melt more resistant to deformation.

Coupling agents can have an effect on viscosity because they influence the interfacial behavior between polymer melt and solid filler. Generally, surface treatment has served to decrease the viscosity and yield stress value compared to untreated fillers, especially at low shear rates [126, 138 - 142]. The coupling agents prevent the fillers from forming aggregates and becoming a strongly interacting network, resulting in a melt which is less resistant to deformation than its uncoupled counterpart. Han and coworkers [140] examined two PP-fiberglass systems (50/50 wt%), one with 1.0 wt% titanate coupling agent (denoted as TTS) and one with no coupling agent. At a shear rate of 100/sec, the addition of TTS to the filled PP reduced the viscosity from $5.2 \cdot 10^{2}$ Pa·sec to $4.5 \cdot 10^{2}$ Pa·sec. This decrease in viscosity was observed over the range of shear rates investigated (70/sec to 400/sec).

Viscosity is not the only material parameter that is affected by the presence of fiber, the first normal stress difference (N_1) is also changed with the addition of fiber. Rigid fibers increase N_1 at both the same shear rate and shear stress [120, 143 - 146]. Czarnecki and White [146] demonstrated this with polystyrene (PS) loaded with 0, 10, and 22 vol% glass fibers. At a shear stress of 10^4 Pa, the unfilled polystyrene had a first normal stress difference of 10^4 Pa, the PS containing 10 vol% glass fiber showed a N_1 of $2 \cdot 10^4$ Pa, and the 22 vol% filled PS had a N_1 of $4 \cdot 10^4$ Pa. For the range of the tests, the PS loaded with 22 vol% glass fiber consistently possessed the highest first normal stress difference.

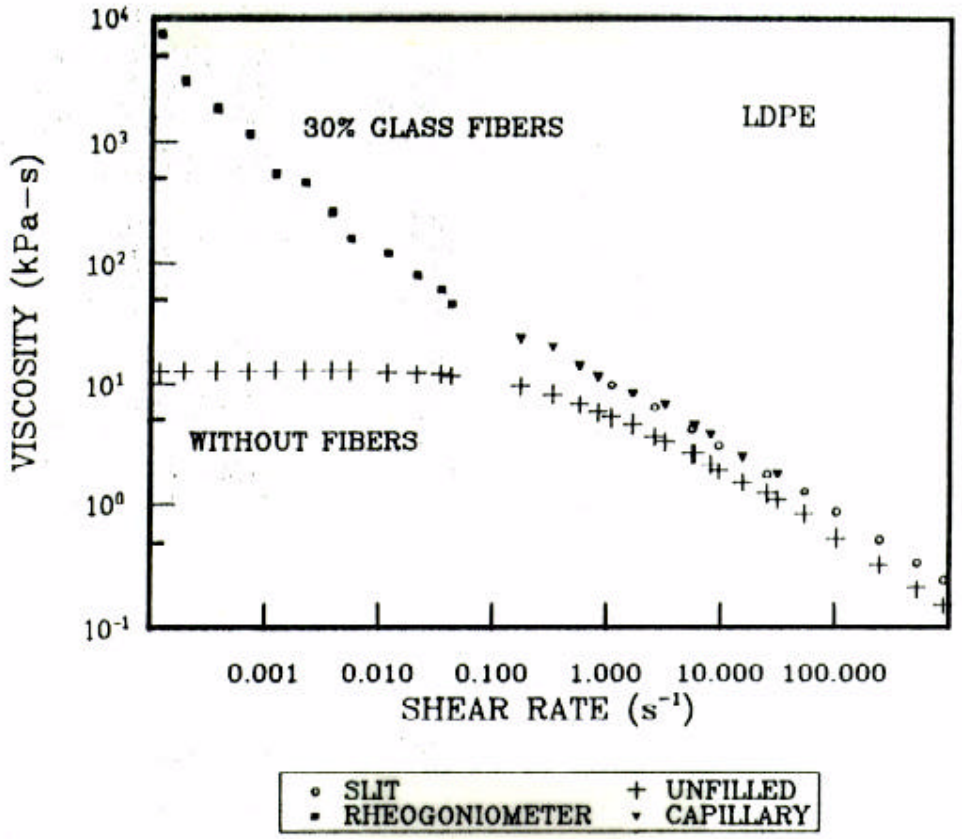

Figure 2.3: Effect of Fiber Concentration on Viscosity. At low shear rates, fiber concentration has a tremendous effect on viscosity because of the influence of fiber-fiber interactions. However, as the shear rate is increased, this influence diminishes because the fibers begin to be aligned in the direction of flow. At sufficiently high shear rates, the alignment is completed and the filled polymer is only moderately more viscous [135].

Another effect observed with the addition of fibers to polymer melts is an increase in the entrance pressure drop [120, 126, 147 - 155]. Crowson and coworkers [151] compared neat polypropylene (PP) to a glass filled PP containing 20 wt% 10 μm diameter fibers and found the fibers always made the entrance effect more pronounced. For instance, a die diameter of 4 mm and a shear rate of 180/sec produced a pressure drop of 110.3 KPa for the neat PP and 689.5 KPa for the filled PP. This is consistent with the observation of higher normal stress differences [126].

Transient behavior is another area which has received some research interest because of the deviations observed from neat resin behavior. One common feature is the presence of large shear stress and first normal stress overshoots which increase with fiber content and aspect ratio [126, 135, 137]. It typically takes 3 to 10 strain units for the stress to reach its maximum and another 50 to 100 strain units to reach steady state. Laun [135] has shown that this transient behavior can be used as a qualitative predictive tool. With a set loading of fiber, as the aspect ratio of the fibers is increased the stress overshoot becomes larger. Substantial differences could be established between aspect ratios as similar as 11, 24, and 27 (shown in Figure 2.4).

2.4.3 Processing Effects on Fiber Reinforcement

Because injection molding pregenerated microcomposites has the potential to provide effective reinforcement, it is necessary to develop some insight on how to maximize mechanical properties. To do this, two areas have received considerable attention: 1) how to retain fiber length and 2) how fiber orientation is developed in filled systems. Both fiber length and orientation is influenced by processing method. This has lead several research groups to investigate how processing variables impact these problems. The subject of fiber orientation is also challenging because of the interrelationship between fiber-fiber contact, the rheological characteristics of the polymer melt, and flow kinematics. By understanding the role of fiber length and orientation on reinforcement, a composite with the highest possible mechanical properties can be created.

2.4.3.1 Processing Effects on Fiber Length

During processing, fiber-filled polymers have the average fiber aspect ratio shortened by the stresses they are subjected to during processing. By studying fiber behavior under different flow conditions, an understanding of how fibers deform and break in viscous melts may be attained. This will provide insight into where fiber breakage is more likely to occur during processing, so adjustments can be made to retain the highest possible aspect ratios. Ultimately, by relating processing conditions to fiber length, the reinforcing capacity of the fiber can be maximized.

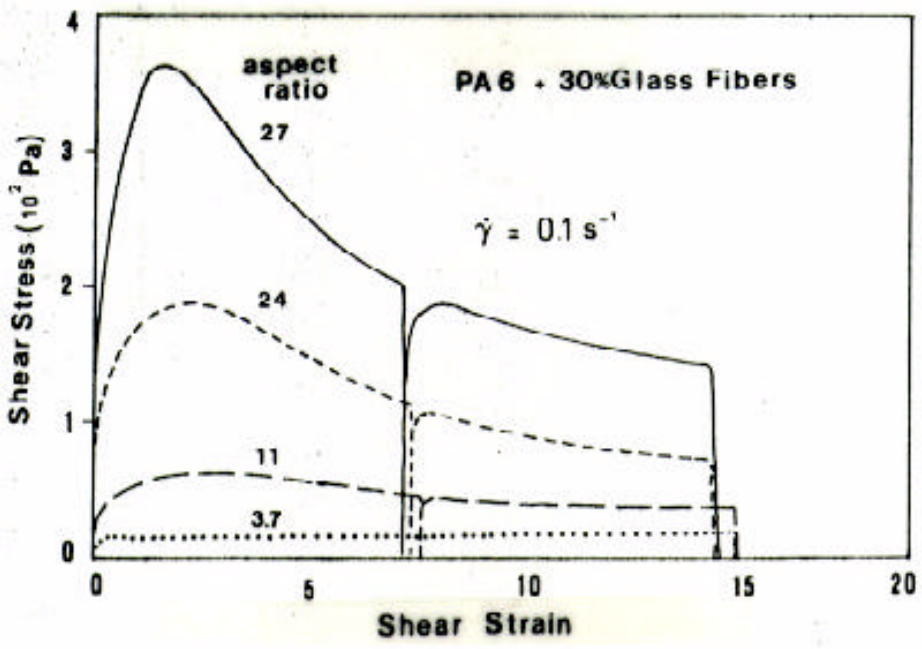

Figure 2.4: Effect of Fiber Aspect Ratio on Transient Rheology. As the aspect ratio of the glass fibers increases, the strain overshoot becomes larger [135]. Note this can be used as a qualitative tool for examining aspect ratio of polymer suspensions.

In attempting to understand how fibers respond to hydrodynamic forces, expressions have been formulated to predict how they bend and fracture. First, with the application of enough axial stress to the fiber, it will begin to bend. Forgacs and Mason [156] derived an equation to predict the critical shear stress for the onset of bending in laminar flow:

$$\text{Equation 2.10: } (\dot{\gamma}\eta)_{bu} = \frac{E[\ln(2L/D) - 1.75]}{2(L/D)^4}$$

where $\dot{\gamma}$ is the shear rate, η is the viscosity of the fluid, E is the bending modulus of the fibers, and L/D is the aspect ratio. Second, if the fiber is bent into a tight enough loop, its tensile strength is exceeded, causing it to fracture. The radius of the tightest possible loop without having the fiber fracture is called the critical radius for breaking (R_b), and this can be determined using thin rod theory [84]:

$$\text{Equation 2.11: } \frac{R_b}{r} = \frac{E}{\sigma_b}$$

For this expression, r denotes the radius of the fiber, E is the Young's modulus, and σ_b is the tensile strength.

Observations made of individual fibers in various flow fields using viscous Newtonian glucose solutions have shown that Equation 2.10 is satisfactory in correlating shear rate to bending modulus [156, 157]. Salinas and Pittman [157] demonstrated this by comparing the flexural modulus of Pyrex glass fibers determined in two ways. First, the flexural modulus was found using a cantilever method, with a 20 mm long fiber being deflected by a small load of known weight. The second method was by applying known shear rates to 12 to 18.7 mm long fibers suspended in glucose solutions. These tests were recorded on video tape to accurately show what shear stress made the fiber bend, with the results applied to Equation 2.10 to calculate the modulus. Comparing the results from these two testing methods is an effective way to evaluate the accuracy of Equation 2.10, because ideally, the flexural modulus should be the same. From the cantilever testing, the experimental modulus was determined to be 52 GPa (± 5.2 GPa), while the value determined from the fiber being in a sheared glucose solution was 81 GPa (± 8.1 GPa). Therefore, the modulus determined through Equation 2.10 is significantly greater than that of the cantilever tests, but does give a fair order of magnitude comparison.

Salinas and Pittman [157] also examined the breaking of glass fibers and compared the experimental results to the theoretically expected results of Equation 2.11. The critical radius for breaking (R_b) was determined for neat strands of glass using thin rod theory. These results were then used to predict what critical stress level would be needed to fracture glass fibers of different aspect ratios. It was found that these predictions correlated well to the experimental results. For example, Pyrex glass fibers with an aspect ratio of 350 were estimated to break at a shear stress equal to $0.35 \cdot 10^{12}$ Pa. Meanwhile,

the experimental results were approximately $0.3 \cdot 10^{12}$, $0.45 \cdot 10^{12}$, $0.6 \cdot 10^{12}$, and $1.25 \cdot 10^{12}$ Pa. Considering the variability in tensile strength, this is good agreement, demonstrating the accuracy of thin rod theory applied to dilute suspensions of glass fibers in Newtonian fluids.

By examining the distribution of fiber lengths, statistics can be used to determine if the fibers are fracturing in the middle or randomly along the length of the fiber. This analysis is based on the idea that the ratio of weight average fiber length to number average fiber length will differ, depending on where the fibers are fracturing:

$$\text{Random Breaking: } \frac{L_w}{L_n} = 2.00$$

$$\text{Breaking in the Middle: } \frac{L_w}{L_n} = 1.44$$

with L_w being the weight average fiber length and L_n the number average length. Initially, this statistical analysis was applied to cellulose fibers [158], with Franzén et al. [84] using it to work with polymer melts. Most of the literature data for extruded or injection molded fiber-filled polymers has an L_w/L_n of about 1.4, showing the fibers are fracturing in half [84]. This is useful because mechanical grinding or fiber-fiber interaction would be expected to cause the fibers to break randomly, giving a L_w/L_n of 2.00. Therefore, the statistical analysis demonstrates that mechanical grinding and fiber-fiber interaction are not the primary means of fracturing the fibers [84].

Fiber length can be lost in four areas in a conventional injection molding process: 1) the solids conveying zone, 2) the melting zone, 3) the melt conveying zone, and 4) the injection phase. Whether damage occurs in each of these zones depends on the brittleness of the fibers, the operating conditions, and the length of the fibers at that stage of the process. Losses in the solids conveying zone would be predominant if there was mechanical grinding as the pellets were being pushed forward [84]. The fibers can be broken in the melting zone if shear forces that exist between the thin pool of melt and the solid pellets are great enough to overcome the fiber's flexural strength [159 - 161]. The same principle applies to the melt conveying zone, because the melt's hydrodynamic forces can bend and fracture the reinforcement, especially for leakage flow over the screw flights [84, 162 - 164]. Also, at this zone the screw has its shallowest channels, producing damaging interactions between the fiber and barrel. If the fibers still have high aspect ratios before being injectioned into the mold, the injection molding phase can apply high shear stresses and fiber-mold interactions which would reduce their length [84, 169 - 174]. With such a wide range of possible causes, studying fiber degradation becomes a complex problem. Exacerbating the issue further is the variability introduced by the various studies using different processing equipment [84, 94]. The shear history exerted on fibers will differ between screw designs and between a batch melt compounder, such as a

Brabender®, and continuous single screw and twin screw devices. This has made much of the work in this area more qualitative than quantitative.

The investigations have indicated that most damage occurs in the melting zone. Lunt and Shortall [159, 160] used fiber filled polyamide 6,6 (PA 6,6, nylon 6,6) to examine the lengths of fibers in this zone. They found that glass fiber in the solid bed had lengths of 2.6 mm, while the melt pool fibers averaged 0.6 mm. Erwin and von Turkovich [161] also noted that in this region the fiber length was significantly lowered. In the single-screw machine they used, they estimated that about a 50% length reduction occurred in this zone. This demonstrates that the thin film between the solid bed and the cylinder appears to be the primary area where the fiber is broken because it is an area of very high shear.

However, fiber damage of similar magnitude has been observed when feeding the fibers directly into the melt [84, 94, 162- 164]. This indicates that the shear forces both in the melting and melt conveying zone can be high enough to cause significant fiber length reduction. In a study by Franzén et al. [84], it was found that dry-blend feeding of aluminum fibers caused the fiber length reduction process to be concentrated in the melting zone of the screw. Meanwhile, when the fiber was added directly to the melt through a feed port, the majority of the breakage occurred close to the feeding point.

Although significant damage to the fibers occurs when they are directly fed into the melt, it has been noted that some of the longer fibers are preserved, thereby improving impact strength. For example, Schweizer [165] compared extrusion compounding versus direct molding to produce PP samples loaded with 20 wt% glass fiber. When a starting fiber length of 6.35 mm was used, extrusion compounding the filled PP before injection molding yielded samples with a number average glass fiber length of 0.686 mm and a notched Izod impact strength of 96 J/m. Meanwhile, when the glass fibers were directly fed into injection molder, the number average length was only slightly higher at 0.711 mm but the composites had a much greater impact strength of 160 J/m. Therefore, even when the quantity of longer fibers was not increased enough to greatly shift the number average fiber length, a significant rise in impact strength was still observed.

Determining the influence of the injection molding phase on breaking of the fiber has been made more complicated because the fiber has been broken apart after being conveyed through the melting and/or melt conveying zones. This often makes the fiber short enough to tolerate the high shear of the injecting step. Therefore, in some studies a conclusive relationship between the injecting step and the effect it had on fiber length was not possible [83, 165].

However, investigations which have avoided this problem have shown that fiber damage in the injection molding phase can not be neglected [84, 89, 115, 166, 167]. In

particular, the influence of nozzle and gate size are important. Small diameter nozzle (< 1 mm) exits create higher shear stresses which may help break any long fibers which reach that point [165, 172]. In fact, nozzle exits of 5.5 mm or larger are recommended for long fiber reinforced thermoplastics, so the reinforcement can proceed into the mold undamaged [115]. Large gate sizes also reduce breakage, as demonstrated in a study which examined this issue [171, 172]. Using PA 6,6 containing 50 wt% long glass fibers, a gate size of 1 mm by 1.5 mm resulted in only 20% of the fibers in the injection molded plaques having lengths greater than 1 mm. Meanwhile, when the melt was processed using gate size of 2 mm by 5 mm, 64% of the fibers were longer than 1 mm. This means that the gate size should not be smaller than 2 mm [171, 172] and in some cases needs to be at least 3 mm [115].

Another factor which can affect fiber length is filler concentration because higher loadings promote more damaging fiber-fiber interactions. Erwin and von Turkovich [161] examined loadings from 1 volume percent (vol%) to 20 vol% and showed no significant reduction in aspect ratio due to the level of loading used. Franzén et al.[84] also showed no effect at volume fractions up to 20% with aluminum, brass, and carbon fiber. However, it has been noted at that higher concentrations, the processed melt has shorter fibers. Stade [162] examined PA 6,6 with loadings of 30 weight percent (wt%) and 50 wt% and noted that at 50 wt% the aspect ratio was lower. Chiu and Shyu [168] observed similar results with polypropylene at 15 and 25 wt%. Therefore, it appears that there reaches a certain concentration where fiber-fiber interaction becomes important. This concentration will grow smaller as the aspect ratio increases [84].

The production and retention of fiber length has also been the subject of some examinations of long fiber reinforced composites [94, 169 - 176]. This form of reinforcement is marketed under the tradename of Verton® and does not use the traditional compounding method to produce fiber-filled pellets. Rather, these long fibers are created through a pultrusion technique which provides a high degree of impregnation without fiber damage. This produces fully wetted fibers equal in length to the pellet length, typically 1.25 cm (0.5 inches) [171]. However, long fibers tend to fracture during injection molding, reducing their length down to some critical minimum value. Because of this, processing variables which are important in retaining fiber size for short fiber reinforced processing are much more important in long fiber processing. If the long fibers are not retained, the pultrusion technique is reduced to just a complicated method of creating short fiber reinforcement.

A thorough study of the effects of processing variables on long-fiber reinforced thermoplastics was undertaken by Cianelli et al. [172]. The variables studied were 1) back pressure, 2) screw rpm, 3) injection pressure, 4) injection speed, 5) screw tip type (fluted channel versus standard), 6) gate size, and 7) screw type (low compression versus a general purpose reciprocating screw). It was found that, when using identical processing

conditions, using a fluted screw tip significantly increased the average fiber length, from 1.8 to 3.7 mm (71 to 144 mils). Creating low-shear conditions by decreasing back pressure, screw rpm, injection pressure, and injection speed also improved the length of the fibers, from an average of 0.64 mm to 2.1 mm. A larger gate size also helped retain fiber length, as shown in a test of 50% long-glass reinforced PA 6,6. A gate size of 1 mm by 1.5 mm gave an average length of 0.49 mm while a 2.0 mm by 5.1 mm gate produced an average length of 1.0 mm. Therefore, to help retain long fibers, it is necessary to use low shear, a fluted screw tip, and large gates. It should also be noted that in order to reduce the effects of the melting zone, the first zone was taken 8°C above the expected melting temperature. This was done to melt the pellets with external heat rather than through viscous dissipation.

2.4.3.2 Processing Effects on Fiber Orientation

Flow kinematics are of paramount importance in producing a part that possesses a planar random orientation of fibers. Investigations into this topic have included both theoretical fiber motion calculations and experimental observations of how fibers have been oriented in injection molded parts. The theoretical studies typically rely on finite element method and Jeffery's theory, which contains several simplifying assumptions that restrict the particle shape, flow environment, and neat fluid viscosity [178]. Solutions obtained in these examinations often qualitatively match what is observed experimentally, but are still incapable of quantitatively predicting fiber orientation [178]. Therefore, the results from simulations can be used to establish trends in orientation, but the data are not accurate enough to confidently state that a part will possess the desired alignment of fibers.

Modeling the injection molding of a fiber filled polymer melt is extremely difficult because the process is transient, nonisothermal, and involves non-Newtonian fluid flow. Often, to simplify the problem, the fiber's presence is decoupled from the fluid's flow by dividing the problem into two parts. First, the flow of the neat resin is modeled to determine the pressure, stress, and velocity fields at each time step in the mold filling process. These results predict the behavior of the melt without any filler. This information is then used *a posteriori*, as data to determine fiber motion in the modeled environment [178]. Jeffery's [177] approach is the one most often used in these simulations, using the following equation of change in fiber orientation:

Equation 2.12: $$\frac{da_2}{dt} = \Omega \cdot a_2 - a_2 \cdot \Omega + \lambda\left(\dot{\varepsilon} \cdot a_2 + a_2 \cdot \dot{\varepsilon} - 2\dot{\varepsilon} : a_4\right)$$

where a_2 is the second order orientation tensor, da_2/dt is the material derivative of the second order orientation tensor, a_4 is the fourth order orientation tensor, Ω is the vorticity tensor, λ is a material constant that depends on the fiber aspect ratio, and $\dot{\varepsilon}$ is the rate of strain tensor. In turn, these variables are represented by the following expressions:

Equation 2.13: $$a_2 = a_{ij} = \int_p p_i p_j \Psi(p,t) dp$$

Equation 2.14: $$a_4 = a_{ijkl} = \int_p p_i p_j p_k p_l \Psi(p,t) dp$$

Equation 2.15: $$\Omega = \Omega_{ij} = \frac{1}{2}\left[\frac{\partial v_j}{\partial x_i} - \frac{\partial v_i}{\partial x_j}\right]$$

Equation 2.16: $$\dot{\gamma} = \dot{\gamma}_{ij} = \frac{1}{2}\left[\frac{\partial v_j}{\partial x_i} + \frac{\partial v_i}{\partial x_j}\right]$$

Equation 2.17: $$\lambda = \frac{\left(r_a^2 - 1\right)}{\left(r_a^2 + 1\right)}$$

where $\Psi(p,t)$ is the fiber probability distribution function, p_i are the components of a unit vector p parallel to the fiber axis, v_i are the components of the velocity vector, x_i are the axes of the coordinate system, and r_a is the aspect ratio of the fiber. The assumptions used in this approach are:

1) the particle shape is ellipsoidal;
2) the particle assumes the velocity of the fluid encapsulating it;
3) away from the particle, the fluid is in steady-state motion. This also means that the volume is considered to be large relative to the particle dimensions;
4) there are no particle-particle interactions;
5) mass and inertia are neglected for both the particle and the fluid;
6) the fluid is Newtonian

Using this formulation, it has been shown that the fiber has no equilibrium position in shearing flow. It rotates rapidly when perpendicular to the flow and slowly when parallel to the flow. This means that most of the fibers are aligned with the flow at any instant and qualitatively matches what is observed in the portion of injection molded parts where shear flow dominates. When Jeffery's approach is applied to elongational flow it shows that the fiber tends to a stable equilibrium position. This has been used to explain why fibers show nearly perfect transverse orientation in the core of center-gated disks [178].

To determine how the assumptions used in Jeffery's theory cause deviations from observed behavior, comparisons have been made between computational simulations and experimental data. It has been found that the ellipsoidal shape can be made equivalent to a

rigid rod by using a factor to determine an equivalent aspect ratio [179, 180]. Assuming that the volume of the surrounding fluid is large relative to the size of the particles is usually not accurate for fiber filled melts. In particular, a nonuniform strain rate and the influence of walls can make this assumption invalid. When wall interference is considered, the fibers move more slowly than the surrounding fluid and rotate more than expected [179, 181, 182]. Particle interactions also cause deviations from Jeffery's theory [179, 183]. Therefore, an additional term must be added to the phenomenological model in order to account for this effect. From these studies, it is clear that the restrictive assumptions can often be modified or taken into consideration so the numerical simulations are in qualitative agreement with experimental observation.

Recently, substantial improvements on predicting fiber orientation have occurred which couple flow and fiber orientation [184 - 189]. The one which shows the best potential centers on the ability to use closure approximations [184]. These numerical techniques approximate the fourth-order moment tensor for fiber orientation in terms of the second-order moment tensor. Cintra and Tucker [184] concluded that the orthotropic closure approximation they used produced errors which are smaller than the typical measurement errors for fiber orientation in reinforced plastics. This means that direct integration of the equation of change for the Cartesian components of the fiber orientation tensor should be accurate enough to model polymer processes. However, computed fiber orientations using this technique has not been compared to experimental observations to confirm this.

Experimental studies of fiber orientation have relied on several techniques, including optical reflection microscopy, contact microradiography, transmission microscopy, and interference contrast light microscopy. The optical reflection technique applied to microtomed samples appears to be the most popular, with several authors determining a three-dimensional fiber orientation by examining the shape of ellipses created when cutting the cross sections of cylindrical fibers [190- 193]. This data has then been used to quantify the orientation. One method employed by Vincent and Agassant [194] is using Herman's orientation function for planar orientation (f_{or}) :

Equation 2.18:

$$f_{or} = \left[2\left\langle \cos^2 \theta \right\rangle - 1\right] / 2 \qquad where \quad \left\langle cos^2 \theta \right\rangle = \left(\sum N_i \cos^2 \theta_i\right) / \sum N_i$$

where θ is the angle relative to a reference direction and N_i is the number of fibers at each angle. The result is a scalar quantity, which some groups have found lacking the descriptive power that a tensorial representation would hold. Advani and Tucker [195] rectified this problem with their formation of a second rank tensor defined by:

Equation 2.19: $a_{11} = \left\langle \cos^2 \theta \right\rangle ; \quad a_{22} = \left\langle \sin^2 \theta \right\rangle ; \quad a_{12} = a_{21} = \left\langle \sin\theta \cos\theta \right\rangle$

These formulas for orientation have been used to show how fiber orientation changes with position in the injection molded plaque, because the orientation on the surface is usually much different than the orientation in the core.

Using microscopy to experimentally determine fiber orientation in center-gated disks, it has been shown that fiber orientation changes dramatically with as one proceeds from the skin to core. The orientation increases to about 0.3 just below the skin and then steadily declines to almost -0.5. A value of -0.5 indicates that all fibers are oriented perpendicularly to the flow direction, and this has been explained as being due to the extensional forces in the hoop direction as the fluid is pushed forward radially. This reemphasizes the efficiency of extensional flows in orienting fibers [194, 196 - 198].

Experimental investigations into fiber orientation of end-gated plaques have also shown the effect of flow kinematics [178, 199, 200]. In one example, a comparison was made between having a runner across the top of the plaque and removing the runner. This changes the flow kinematics and was suspected to have an effect on fiber orientation. The effect was confirmed, with the runnerless plaque having more fibers oriented perpendicular to the flow direction for a longer distance down the length of the plaque. It was also observed that both plaques appeared to reach a critical minimum value where the size of the core leveled off [178] (shown in Figure 2.5).

To help control fiber orientation and eliminate the problem of weld lines, a novel processing method has been developed [175, 201- 207]. This has been termed shear controlled orientation technology (Scortec®) and is called Scorim® when applied to injection molding. It operates on the principle that after the mold is filled, if the polymer is not allowed to immediately solidify subsequent shearing steps can be used to orient the fiber. This shearing is provided by using sets of pistons which pump the fluid as solidification is allowed to occur. The result is successive layers of polymer can be oriented in different directions to produce an isotropic part (see Figure 2.6 for a diagram of the process) . Allan and Bevis [201 - 203] have examined Scorim technology applied to glass reinforced polypropylene and liquid crystalline polymers [207]. For glass reinforced polypropylene, they found that it was possible to form 0-90° laminates as well as uniaxially aligned fibers, depending on the arrangement and operation of the reciprocating pistons.

Applied to pregenerated microcomposites, it would be expected that some differences in orientation would occur compared to the other forms of reinforcement. One reason to suspect this is due to the difference in fiber diameter. TLCP fibers can be over an order of magnitude smaller than glass fiber, so they may be affected by the mold geometry differently. In cases where fiber-wall interactions are important for glass fibers, TLCP fibrils may be too small for it to be of any significance. Also, smaller diameter

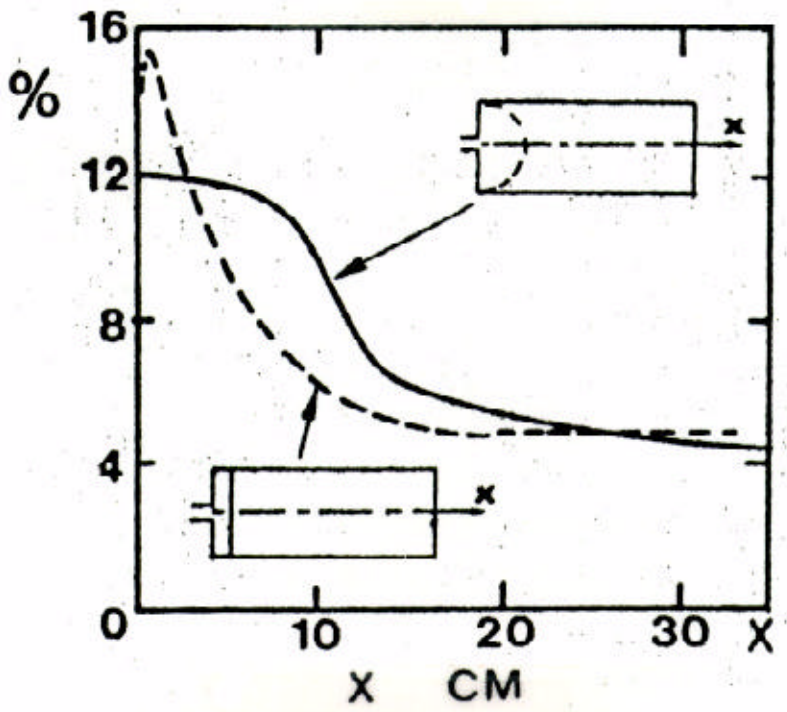

Figure 2.5: Effect of End Gate Geometry on Fiber Orientation. Using a film gate versus a point gate shows the influence of flow history on fiber orientation, with the core region having orientation perpendicular to the flow direction [178]. This also shows that as the distance from the gate increases, the core region decreases because of an absence of elongational forces.

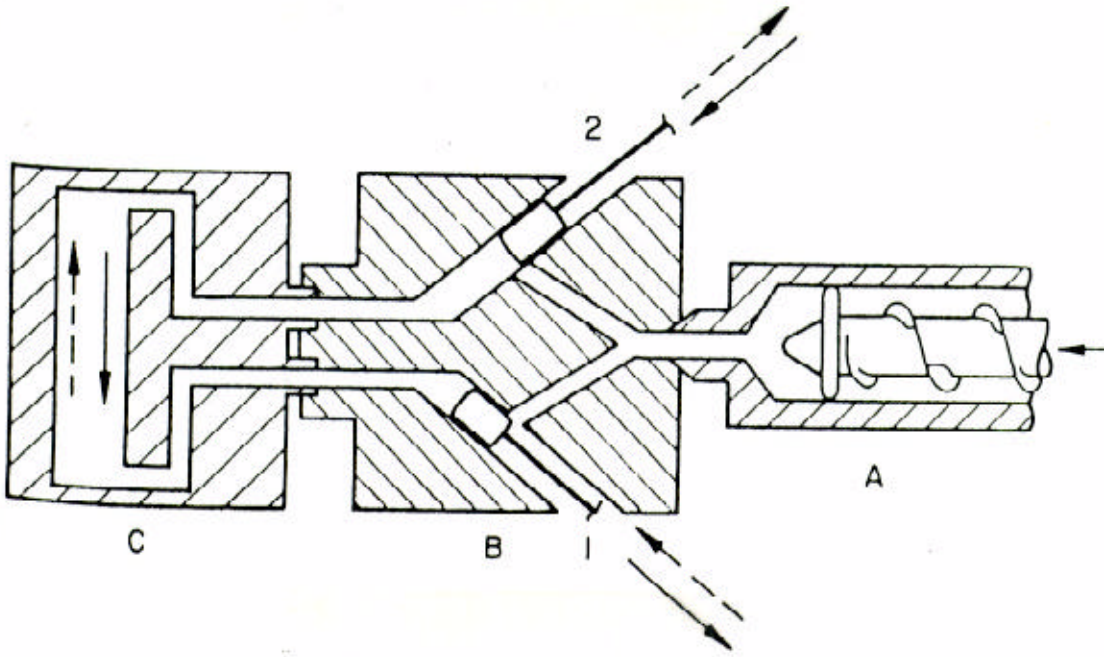

Figure 2.6: Diagram of the Scorim® Process. This figure illustrates how the Scorim process succeeds in orienting polymer melt in the mold [175].

fibers mean a higher number are present per unit volume. Therefore, more fiber-fiber interaction would occur, which can affect the final orientation in the injection molded plaque [119]. In simulations, these interactions are accounted for with a rotary diffusion term [184]. Lastly, the TLCP fibrils are being processed above their glass transition temperature. This may make them behave more like aramid fibers, which tend to kink and bend more readily rather than break when subjected to shear, resulting in more isotropic mechanical properties [88, 113, 171, 172].

The summary of processing effects on fiber reinforcement focused on fiber size and fiber behavior in a fluid medium because of their influence on producing high mechanical properties in injection molded composites. In particular, fiber breakup and orientation are two key issues which determine these properties. It appears that fiber breakup occurs mainly in the melting and melt conveying zones, although long fiber reinforcement can experience significant reductions in aspect ratio during the mold filling step. Therefore, to minimize the fracturing of fiber reinforcement, it is necessary to subject the fibers to low shear stresses and use a fluted screw tip. Meanwhile, how fiber orientation is developed in injection molded parts is still not understood well enough to be accurately predicted through computer modeling. Therefore, fiber orientation is still determined by using microscopy. Once the fiber orientation for a part has been determined, a distribution orientation function can be used with composite theory to predict the mechanical properties of the injection molded part.

2.4.4 Mechanical Properties of Fiber Reinforced Thermoplastics

The main reason for compounding fiber into thermoplastics is to improve mechanical properties. However, several questions arise in this regard. How much of an improvement is realized at different loading levels? The previous section showed that changing the processing conditions yields different aspect ratios and different orientations. How does this change affect the mechanical properties of the composite? What properties do long fiber reinforcement and the Scorim technology provide compared to conventional short fiber reinforcement? These are important questions which need to be answered for a complete comprehension of fiber reinforced polymer behavior.

Fiber loading levels can have a significant effect on mechanical properties, with higher concentrations of fiber providing an increase in modulus and strength. In general, loadings are typically in the 20-30 wt% range, with loadings up to 50% commercially available [89]. As the level of reinforcement is increased, the mechanical properties also rise, but this is not a linear relationship [79]. An excellent investigation of how loading level affects reinforcement was undertaken by Hiscock and Bigg [208] for reinforced polyamide 6 (PA6, nylon 6). Loadings of 10 and 25% were studied, using different types

of glass fiber and various effects of silane treatment. Type H fibers were typical of the results produced, with 10 wt% glass fiber in PA6 having a tensile strength of 101 MPa and a modulus of 5.10 GPa while PA6 with 25 wt% glass possessed a strength of 169 MPa and a modulus of 11.1 GPa. These results show that increasing the loading by two and one-half times does not produce a commensurate increase in any of the mechanical properties. This should be expected, because as the concentration of fiber increases, it allows more fiber-fiber interactions which decrease the average fiber size. Smaller fiber aspect ratios increase the importance of stress concentration at the fiber ends, resulting in earlier failure and lower mechanical properties.

Another study relating loading level, mechanical properties, and efficiency of reinforcement was performed by Xavier and Misra [209]. Polypropylene was loaded with 10, 20, 28, and 35 wt% glass and injection molded into ASTM standard tensile bars. As the loading was increased from 10 to 35 wt%, the tensile modulus rose from 1.59 to 3.41 GPa. Meanwhile, the average fiber length decreased from 0.55 mm to 0.35 mm and the efficiency of reinforcement decreased from 0.26 to 0.22. This again confirms the relationship that higher loadings produce both lower fiber lengths and a lower efficiency of reinforcement.

Using smaller diameter fibers can also influence final mechanical properties [210, 211]. Watkins et al. [212] studied glass fibers with diameters from 13.5 μm to 6.5 μm blended in polyamide 6,6 (PA 6,6, nylon 6,6), poly(butylene terephthalate) (PBT), poly(ether ether ketone) (PEEK), polycarbonate (PC), and poly(ether imide) (PEI) at loadings from 20 to 40 wt%. All materials were injection molded into ASTM test specimens, which were tested for tensile strength and unnotched impact strength. For every weight fraction of glass, both the tensile strength and impact strength was higher when smaller diameter fibers were used. A typical example is with PA 6,6 at 30 wt%. This showed an increase in tensile strength from 176.6 MPa to 198.7 MPa and in impact strength from 811.7 J/m to 1233 J/m, establishing a strong relationship between smaller fiber diameter and higher mechanical properties (refer to Table 2.2).

However, this relationship may not hold for very small fiber diameters. There may be an optimum fiber size to attain the highest possible mechanical properties. In another study, fibers with diameters of 13, 7, 4, and 0.5 microns were used in a PA 6,6 matrix [213]. This investigation showed optimal properties at 7 μm, with 4 μm giving properties equal to the 13 μm fibers and 0.5 μm fibers yielding the lowest tensile and flexural values, as shown in Figure 2.7.

It was speculated that the existence of an optimum fiber size is due to two competing relationships. Loading polymer melt with fibers having smaller diameters results in a larger number of fibers in the melt at the same weight fraction. For example,

Table 2.2: Effect of Fiber Diameter on Mechanical Properties. Fiber types used in this study were DE (6.5 μm), G (10 μm), and K (13.5 μm). For both the tensile and impact strengths, significant improvements were noted when smaller diameter fibers were used [212].

Tensile Strength (MPa)

Glass Loading	20 wt%			30 wt%			40 wt%		
Fiber Dia.	DE	G	K	DE	G	K	DE	G	K
PA6,6	169.7	162.2	146.9	198.7	188.4	176.6	221.	213.9	202.9
PBT	122.8	115.2	107.6	143.5	132.5	124.2	153.9	140.8	131.8
PEEK	147.7	145.6	137.3	166.9	166.3	159.4	***	169.7	170.4
PC	126.9	123.5	111.8	152.5	140.8	131.8	176.6	164.2	151.8
PEI	133.3	127.7	120.1	161.5	147.7	140.8	***	156.6	151.1

Unnotched Impact Strength (J/m)

Glass Loading	20 wt%			30 wt%			40 wt%		
Fiber Dia.	DE	G	K	DE	G	K	DE	G	K
PA6,6	934.5	784.9	608.8	1233	1116	811.7	1329	1169	982.6
PBT	806.3	694.2	539.3	811.7	688.9	624.8	720.9	672.8	587.4
PEEK	747.6	726.2	683.5	640.8	683.5	678.2	***	512.6	582.1
PC	742.3	694.2	795.7	768.9	715.6	838.4	736.9	699.5	795.7
PEI	411.2	373.8	411.2	427.2	368.5	386.5	***	363.1	363.1

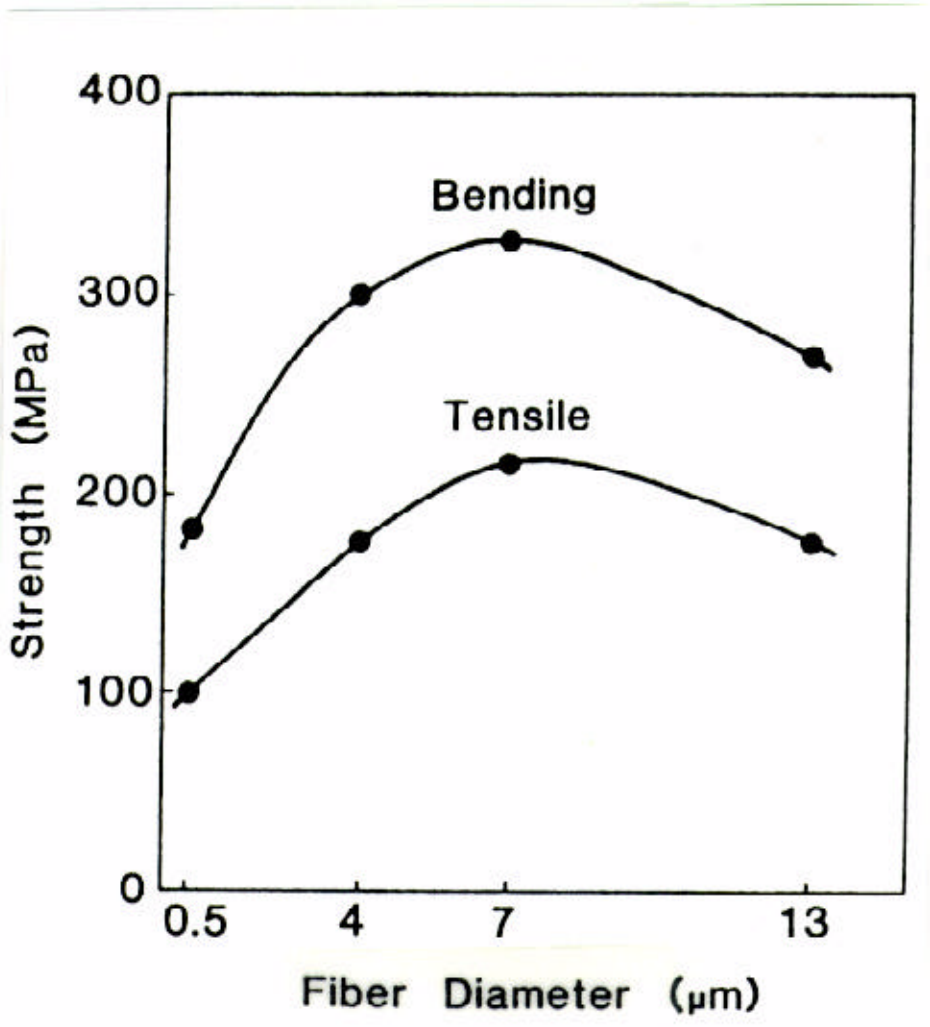

Figure 2.7: Possible Existence of a Optimal Fiber Diameter. Examining bending and tensile strengths of PA 6,6 (30 wt% glass), it appears that a fiber diameter of 7 μm provides the best mechanical properties [213].

the number of 6.5 μm diameter filaments would be four times the number of 13 μm diameter fibers at the same weight fraction of reinforcement. This provides more surface area per unit volume of reinforcement, which is beneficial because of the potential for better stress transfer. However, having more fibers also means having more fiber ends, which serve as stress concentrators and lower mechanical properties [89]. Therefore, there may exist a fiber diameter which maximizes the benefits of high surface area while minimizes the detrimental effects associated with the number of fiber ends.

Fiber length has a substantial effect on mechanical properties, with longer fibers providing more reinforcement to the matrix. The best illustration of this is provided by comparing short fiber reinforcement with long fiber reinforcement [171, 172]. Using PA 6,6 with 50 wt% glass loading, the short glass fiber had an average length of 0.33 mm while the long fiber had an average length of 2.9 mm. The higher aspect ratios of the long fiber reinforcement consistently provided mechanical properties superior to those measured from short fiber reinforced composites. The most dramatic improvement was observed in notched Izod testing, where the impact strength was 261 J/m for the long fiber case and 139 J/m for short fiber reinforcement. Table 2.3 shows the magnitude of improvement, revealing that although all mechanical properties are affected by fiber size, impact properties appear to be especially sensitive to the length of the reinforcing fibers.

In order to accurately correlate mechanical properties to fiber alignment, it is necessary to produce composite plaques where the fiber alignment has been well controlled. Often, this is accomplished by compression molding plaques using strands with a high degree of uniaxial alignment. For example, McNally [214] extruded 30 wt% glass-reinforced PBT to obtain highly oriented strands. After confirming that the glass was highly oriented by using scanning electron microscopy, the strands were then uniaxially compression molded into plaques. The plaques were cut at angles of 0°, 22 ½°, 45°, 67 ½°, and 90° with respect to the fiber orientation to determine how tensile properties changed. The tensile strength, tensile modulus, flexural strength, and flexural modulus were all observed to decrease by about one-half as the testing proceeded to 90° alignment. Impact testing was even more sensitive to fiber alignment. The highest notched Izod impact strength was 69.9 J/m while the lowest was 32.5 J/m. The reversed notched Izod tests showed similar results, with an impact strength of 265 J/m when the fibers were at a fiber orientation angle of 0°, while just 99.8 J/m when the fiber orientation angle was 90°.

Blumentritt et al. [215, 216] also investigated compression molded samples, comparing random alignment with uniaxial alignment using a variety of different resins,types of fiber, and loading levels. These studies showed that with glass fiber, a random-in-plane alignment gave significantly lower tensile properties, but the magnitude of the decrease varied from material to material. For instance, loading high density polyethylene (HDPE) with 20 vol% glass produced composites with a tensile strength of

Table 2.3: Short Fiber versus Long Fiber Mechanical Reinforcement. Two sets of injection molded samples of glass fiber-filled polyamide 6,6 (nylon 6,6) (50 wt% glass) were tested for mechanical properties, with the only difference between the two sets being the fiber length of the reinforcement. The results from these tests demonstrated that when the long glass fiber aspect ratio was retained, tensile, flexural *and* impact properties were improved. [171, 172].

	Tensile Str. (MPa)	Flexural Str. (MPa)	Flexural Mod. (GPa)	Notched Impact Str. (J/m)	Unnotched Impact Str. (J/m)	Dart Drop (J)
Short Glass	210	323.1	12.3	139	1230	7.9
Long Glass	246	351.4	14.1	261	1790	10.6

142.7 MPa in unidirectional alignment but only 42.13 MPa in the random mode. Meanwhile, polycarbonate using the same vol% glass had tensile strengths of 114.4 MPa and 61.36 MPa under the same two methods of alignment [215]. This indicates fiber alignment is not the only factor which affects mechanical performance; interfacial adhesion and how the fiber influences matrix properties may also have a significant effect.

The influence of interfacial adhesion on the mechanical properties of glass fiber-filled PA6 was examined by Bader and Collins [217]. The test samples were prepared by injection molding, using both an end-gated as well as a side-gated test bars. For dry end-gated samples containing 25 wt% glass fibers (12 μm in diameter), one set possessed fibers coated with a silane coupling agent while the second was not. The coated glass had a tensile modulus of 11.1 GPa, a tensile strength of 169 MPa, a notched Charpy impact energy of 19.7 KJ/m^2, and an interfacial shear strength of 44 MPa. Meanwhile, the glass fibers without the silane coupling agent possessed lower mechanical properties, with a stiffness of 10.7 GPa, a strength of 102 MPa, an impact energy of 16.8, and an interfacial shear strength of 35 MPa. These results demonstrate that interfacial adhesion can play an important role in maximizing mechanical properties.

One investigation which examined the influence of flow kinematics on the mechanical properties of filled polymers was undertaken by Darlington et al. [218], using an end-gated circular disk. The diameter and thickness of the disk was varied to determine the effect those parameters would have on mechanical behavior. It was found that making the disk thinner caused less mechanical anisotropy and that increasing the diameter both reduced anisotropy and improved the measured properties significantly. They attributed this to a balance between the fiber orientation in the core and the surface, with the core's orientation being transverse to the major flow direction. It was also noted that in order to create this balance, the flow behavior of the fluid had to be considered.

Pipes and coworkers [219] molded end gated tensile bars for their examinations of fiber orientation. The bars were then cut into different sections to examine how the orientation in each layer is reflected in mechanical properties. The edge section was determined to have an orientation parameter of 0.8 and the core a parameter of -0.5. The edge showed a longitudinal tensile modulus of 18.3 GPa and a transverse modulus of 9.0 GPa while the core had moduli of 9.9 GPa and 15.2 GPa in the same two directions. This again shows that the flow kinematics creates fiber orientation in the bars and the change in orientation through the thickness has a measurable effect on mechanical properties. Notch sensitivity between the two sections was determined by drilling holes of different diameters through the test samples. It was found that the more highly oriented skin section was more sensitive to the holes, indicating that strength reduction between machined notches and molded notches will not be equivalent.

A study of center-gated disks was undertaken by Kessler [89], which investigated flexural properties. For neat PA 6,6, the flexural strength and modulus were equivalent for the directions parallel and perpendicular to the radial flow direction. Adding 30 wt% glass fiber had a dramatic effect, with the parallel flexural strength being 239 MPa while the perpendicular flexural strength was just 177 MPa. A similar effect was observed with the flexural modulus.

Because conventional injection molding produces a dramatic difference in skin and core fiber orientation, Scorim technology has been developed as a method to control fiber alignment. Gibson and coworkers [204] demonstrated its ability using a high temperature cure dough molding compound containing 15 wt% glass fibers. The dough molding compound consisted of 17 wt% polyester resin, 7 wt% low profile additive, 59 wt% filler, 1.75 wt% zinc stearate release agent, 0.4 wt% dicumyl peroxide initiator, and 15 wt% E glass fibers. Tensile bars molded using this technique showed higher tensile and flexural strengths as the melt was subjected to more oscillations from the pistons, with small improvements in moduli also noted. For instance, the flexural strength of samples molded conventionally was 49 MPa, while after 30 oscillations using the multiple live-feed injection molding process (MLFIM) the strength rose to 65 MPa. They attributed the improvement in mechanical properties to the MLFIM and its ability to control the alignment of the fiber reinforcement (additional mechanical properties on Figure 2.8).

The primary areas of concern in fiber-filled polymers have been examined. Rheology, processing effects on fiber reinforcement, and mechanical properties have been discussed, with special focus placed on glass fibers. From this review, it has been shown that rheological testing is a useful qualitative method of determining fiber aspect ratio and size, as well as providing the melt viscosity which will be encountered in processing. Proper processing of filled systems can help retain high fiber aspect ratio and produce the desired fiber alignment. In particular, to prevent fiber damage, any steps which can be taken to avoid or minimize the high shear in the melting and melt conveying zones should be attempted. Only by taking the processing effects into account can mechanical properties be maximized and the fullest reinforcing ability of the fibers be utilized.

2.5 Research Objectives

The topics reviewed in the previous sections were chosen specifically to address key concerns in this research. To assist in understanding the scope of this work, the major points from this literature review will be briefly delineated. After providing this synopsis, a statement of the research objectives will be given. This will be proceeded with a brief accounting of supplemental work which will be necessary to fulfill these objectives.

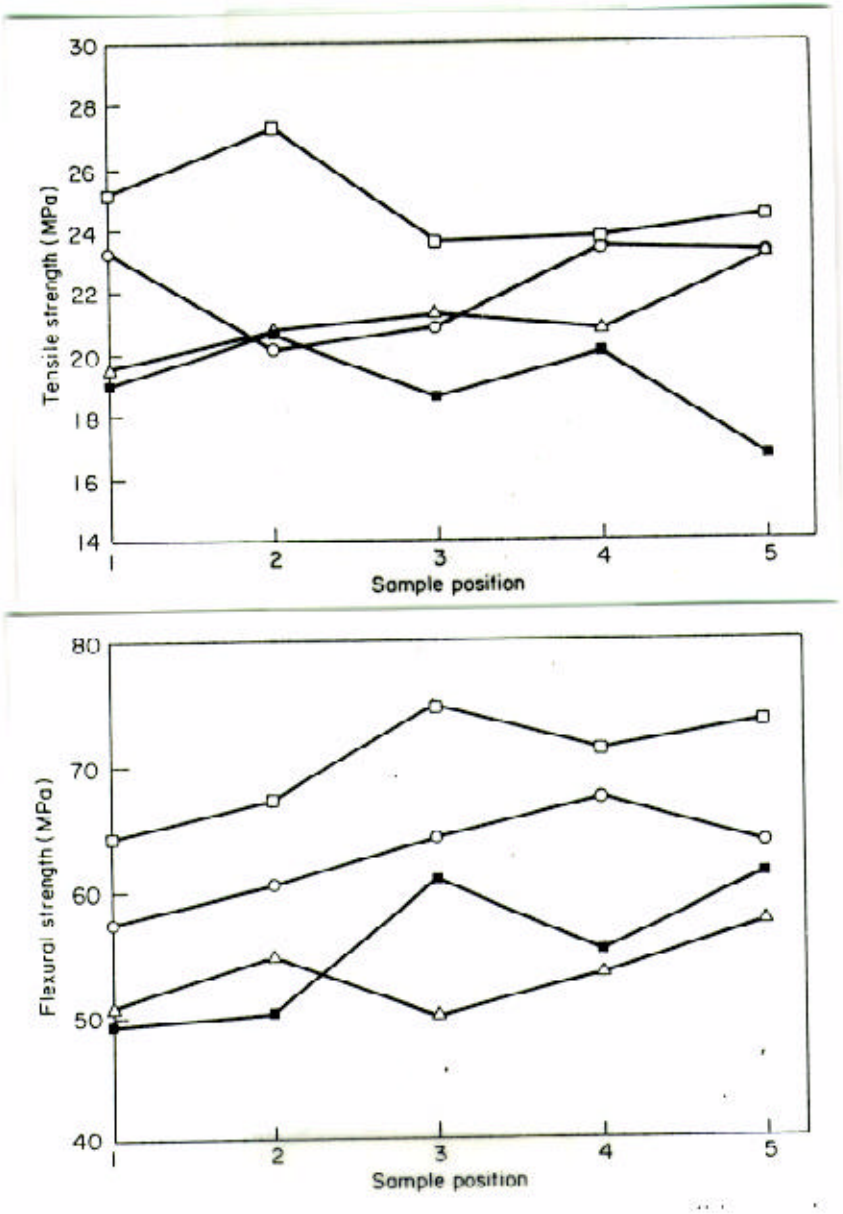

Figure 2.8: Scorim Technology Improves Tensile and Flexural Strength. Mechanical properties of single gated moldings are shown, using a dough molding compound with 15 wt% glass fibers [204]. Processing Conditions: ■ : static, △ : 10 oscillations, ○ : 20 oscillations, □ : 30 oscillations.

The first attempts to utilize TLCPs mechanical properties were done by making in situ composites, but these composites showed extreme anisotropy and did not fully utilize the TLCP as a reinforcing phase. Attempts to solve these problems in the injection molding process have met little success. This is due to the nature of the mold filling process, where high molecular orientation and long, slender fibrils are only created where the melt is subjected to extensional deformation.

Another approach to the problem of anisotropy has been to divide the processing into two steps: 1) create the in situ composite and 2) form the composite into the desired shape. By injection molding this form of fiber reinforcement, the potential exists to provide the desired combination of fast cycle times, the ability to form complex, less anisotropic parts, and retention of high mechanical properties from the TLCP orientation step. Therefore, this processing scheme has the potential to overcome the difficulties associated with in situ composites while retaining the beneficial characteristics of the TLCP phase.

The process of injection molding pregenerated microcomposites has several advantages over conventional, short fiber forms of reinforcement. The TLCP fibrils are an order of magnitude smaller in diameter, so the reinforcing phase can be shorter and still possess a high aspect ratio. Their density is lower than the other forms of reinforcement, making their specific modulus and specific strength values higher than glass and providing the potential for a lighter weight composite. Also, the TLCP fibrils are fully wetted by the spinning process, which avoids the compounding step that is necessary for other injection molding methods.

Injection molding of pregenerated microcomposites has shown the ability to reduce anisotropy, but several questions still remain. It has not been shown that this processing scheme can be applied to matrix/TLCP blends besides those using polypropylene as the matrix. The previous research with injection molded pregenerated microcomposites showed mechanical properties below their theoretical maximum. The explanation for this has been incomplete, with agglomeration, loss of fibril aspect ratio, and molecular relaxation being cited as possible causes. Also, the research on pregenerated microcomposites has not used matrix/TLCP fibers which have the maximum possible properties. Therefore, a comprehensive comparison of the effect of fiber draw ratio on pregenerated microcomposite mechanical properties has not been performed. It is also worth noting that no work has been done to determine if the supercooling/crystallization behavior of TLCPs can be tailored for this process, which would potentially expand the number of matrix/TLCP composite systems that could be explored.

From these questions, the objectives of this research are:

1. **Demonstrate that poly(ethylene terephthalate) (PET) can be used in the pregenerated microcomposite process without losing the reinforcing ability of the TLCP fibrils. This includes finding an appropriate TLCP suitable for processing with PET.**

2. **Perform a comprehensive study of the pregenerated microcomposite process to determine where property losses are occurring. Develop processing options to overcome these problems.**

3. **Determine the effect of fiber draw ratio on mechanical properties by using fibers with optimal mechanical properties.**

4. **Determine if the crystallization/supercooling behavior of a high melting point TLCP can be modified by melt blending with a second, lower melting point TLCP.**

2.6 References

1 A. Siegmann, A. Dagan, and S. Kenig, *Polymer*, 26, 1325 (1985).
2 K.G. Blizard and D.G. Baird, *SPE ANTEC Tech. Papers*, 32, 311 (1986).
3 A.I. Isayev and M.J. Modic, *SPE ANTEC Tech. Papers*, 32, 573 (1986).
4 A.I. Isayev and M.J. Modic, *Polym. Comp.*, 8 (3), 158 (1987).
5 A.I. Isayev and S. Swaminathan, in *Proceedings of the 3rd Annual Conference on Advanced Composites*, 259 (1987).
6 R. Ramanathan, K.G. Blizard, and D.G. Baird, *SPE ANTEC Tech. Papers*, 33, 1399 (1987).
7 G. Kiss, *Polym. Eng. Sci.*, 27 (6), 410 (1987).
8 W. Brostow, T.S. Dziemianowicz, J. Romanski, and W. Werber, *Polym. Eng. Sci.*, 28 (12), 785 (1988).
9 Y. Oyanagi, I. Sekiguchi, and K. Kubota, in *Proceedings of the 1st Japan International SAMPE*, 633 (1989).
10 W. Pfandl and L. Yin, *AMSE Polymeric Materials Science and Engineering (Proceedings of the ACS): Division of Polymeric Materials: Science and Engineering*, 60, 634 (1989).
11 P.R. Subramanian and A.I. Isayev, *SPE ANTEC Tech. Papers*, 36, 489 (1990).
12 G. Crevecouer and G. Broeninckx, *Polym. Eng. Sci.*, 30 (9), 532 (1990).
13 W. Brostow, T.S. Dziemianowicz, M. Hess, and R. Kosfeld, in *Liquid Crystalline Polymers - ACS Symposium Series (Vol. 435)*, 402 (1990).
14 T. Limtasiri and A.I. Isayev, *J. Appl. Polym. Sci.*, 42, 2923 (1991).

15 A. Metha and A.I. Isayev, *Polym. Eng. Sci.*, 31 (13), 971 (1991).
16 C. Carfagna, E. Amendola, L. Nicolais, D. Acierno, O. Francescangeli, B. Yang, and R. Rustichelli, *J. Appl. Polym. Sci.*, 43, 839 (1991).
17 M.S. Silverstein, A. Hiltner, and E. Baer, *J. Appl. Polym. Sci.*, 43, 157 (1991).
18 A. Datta, J.P. de Souza, A.M. Sukhadia, and D.G. Baird, *SPE ANTEC Tech. Papers*, 37, 913 (1991).
19 D. Dutta, R.A. Weiss, and K. Kristal, *Polym. Comp.*, 13 (5), 394 (1992).
20 M.T. Heino and J.V. Seppälä, *Intl. J. Mat. and Prod. Tech.*, 7 (1), 56 (1992).
21 F.P. La Mantia, A. Valenza, and P.L. Magagnini, *J. Appl. Polym. Sci.*, 44, 1257 (1992).
22 T. Harada, K. Tomari, A. Hamamoto, S. Tonogai, K. Sakaura, S. Nagai, and K. Yamaoka, *SPE ANTEC Tech. Papers*, 38, 376 (1992).
23 A. Golovoy, M. Kozlowski, and M. Narkis, *Polym. Eng. Sci.*, 32 (13), 854 (1992).
24 J. Seppälä, M. Heino, and C. Kapanen, *J. Appl. Polym. Sci.*, 44, 1051 (1992).
25 H.J. O'Donnell, A. Datta, and D.G. Baird, *SPE ANTEC Tech. Papers*, 38, 2248 (1992).
26 R.E.S. Bretas and D.G. Baird, *SPE ANTEC Tech. Papers*, 38, 5233 (1992).
27 R.E.S. Bretas and D.G. Baird, *Polymer*, 33 (24), 5233 (1992).
28 M.T. Heino, in *Polymer Technology Publication Series No. 14*, National Technical Information Service, Springfield (VA), 1993.
29 M.T. Heino and J.V. Seppälä, *J. Appl. Polym. Sci.*, 48 (9), 1677 (1993).
30 F.P. La Mantia, F. Cangialosi, U. Pedretti, and A. Roggero, *Eur. Polym. J.*, 29 (5), 671 (1993).
31 D. Dutta, R.A. Weiss, and K. Kristal, *Polym. Eng. Sci.*, 33 (13), 838 (1993).
32 H.J. O'Donnell, A. Datta, and D.G. Baird, *SPE ANTEC Tech. Papers*, 39, 2248 (1993).
33 D.G. Baird, S.S. Bafna, J.P. de Souza, and T. Sun, *Polym. Comp.*, 14 (3), 214 (1993).
34 A. Datta, H.H. Chen, and D.G. Baird, *Polymer*, 34 (4), 759 (1993).
35 S.S. Bafna, J.P. de Souza, T. Sun, and D.G. Baird, *Polym. Eng. Sci.*, 33 (13), 808 (1993).
36 S.S. Bafna, T. Sun, and D.G. Baird, *Polymer*, 34 (4), 708 (1993).
37 K.T. Teh, J. Morton, J.P. de Souza, and D.G. Baird, in *Ninth International Conference on Composite Materials (Madrid, Spain)*, 1993.
38 H.J. O'Donnell, A. Datta, and D.G. Baird, in press.
39 H.J. O'Donnell, PhD Dissertation, Virginia Polytechnic Institute and State University, Blacksburg (VA), 1994.
40 H.J. O'Donnell and D.G. Baird, *Polym. Eng. Sci.*, 36 (7), 963 (1996).
41 H.J. O'Donnell and D.G. Baird, *Intl. Polym. Proc.*, XI (3), 1 (1996).
42 H.J. O'Donnell and D.G. Baird, *Polymer*, 36 (16), 3113 (1995).
43 L.-M. Sun, T. Sakamoto, S. Ueta, K. Koga, and M. Takayangi, *Polym. J.*, 26 (8), 939 (1994).

44 L.-M. Sun, T. Sakamoto, S. Ueta, K. Koga, and M. Takayangi, *Polym. J.*, 26 (8), 953 (1994).
45 L.-M. Sun, T. Sakoda, S. Ueta, K. Koga, and M. Takayangi, *Polym. J.*, 26 (8), 961 (1994).
46 G.O. Shonaike, H. Hamada, S. Yamaguchi, M. Nakamichi, and Z. Maekawa, *J. Appl. Polym. Sci.*, 54, 881 (1994).
47 Y. Yang, J. Yin, B. Li, G. Zhuang, and G. Li, *J. Appl. Polym. Sci.*, 52, 1365 (1994).
48 K. Engberg, M. Ekblad, P.E. Werner, and U.W. Gedde, *Polym. Eng. Sci.*, 34 (17), 1346 (1994).
49 B.C. Kim and S.M. Hong, *Mol. Cryst. Liq. Cryst.*, 254, 251 (1994).
50 R.M. Holsti-Miettinen, M.T. Heino, and J.V. Seppälä, *J. Appl. Polym. Sci.*, 27 (5), 573 (1995).
51 A. Datta and D.G. Baird, *Polymer*, 36 (3), 505 (1995).
52 L.M. Smartt and D.G. Baird, *SPE ANTEC Tech. Papers*, 41 (II), 1428 (1995).
53 L.M. Smartt, unpublished data.
54 J.P. de Souza and D.G. Baird, *Polymer*, 37 (10), 1985 (1996).
55 S.C. Tjong, J.S. Shen, and S.L. Liu, *Polym. Eng. Sci.*, 36 (6), 797 (1996).
56 S.C. Tjong, S.L. Liu, and R.K.Y. Li, *J. Mat. Sci.*, 31 (2), 479 (1996).
57 H.J. O'Donnell, H.H. Chen, and D.G. Baird, *SPE ANTEC Tech. Papers*, 39, 1711 (1993).
58 S. Kenig, *Polym. Eng. Sci.*, 29 (16), 1136 (1989).
59 G.G. Viola, D.G. Baird, and G.L. Wilkes, *Polym. Eng. Sci.*, 25 (14), 888 (1985).
60 D.E. Turek and G.P. Simon, *Polymer*, 34 (13), 2750 (1993).
61 K.G. Blizard and D.G. Baird, *Polym. Eng. Sci.*, 27 (9), 653 (1987).
62 D.G. Baird and R. Ramanathan, in *Contemporary Topics in Polymer Science (Vol. 6)*, ed. B.M. Culbertson, Plenum Press, New York 1989.
63 K. Fujiwara, M. Takahashi, and T. Asuda, *Intl. Polym. Proc.*, 6 (3), 232 (1991).
64 S.K. Garg and S. Kenig, in *High Modulus Polymers*, ed. A.E. Zachariades and R.S. Porter, Marcel Dekker, New York 1988.
65 Z. Tadmor, *J. Appl. Polym. Sci.*, 18, 1753 (1974).
66 G.I. Taylor, *Proc. Roy. Soc.*, A146, 501 (1934).
67 W. Hufenbach and M. Lepper, *Mat. Sci. Forum*, 157-162, 1593 (1994).
68 R.P. Mozes, *SPE ANTEC Tech. Papers*, 38, 1259 (1992).
69 T. Brinkmann, P. Hoeck, and W. Michaeli, *SPE ANTEC Tech. Papers*, 37, 1857 (1991).
70 A.A. Handlos, *PhD Dissertation*, Virginia Polytechnic Institute and State University, Blacksburg (VA) 1994.
71 A.A. Handlos and D.G. Baird, *Intl. Polymer Proc.*, 11(1), 1 (1996).
72 A.A. Handlos and D.G. Baird, *Polym. Compos.*, in press.
73 M.T. Heino, T.P. Vainio, and J.V. Seppälä, *Polym. and Polym. Comp.*, 1 (6), 439, (1993).

74 M.A. McLeod and D.G. Baird, *SPE ANTEC Tech. Papers*, 41 (II), 1420 (1995).
75 A.A. Handlos, E.A. Sabol, and D.G. Baird, *SPE ANTEC Tech. Papers*, 40 (II), 1594 (1994).
76 A.A. Handlos and D.G. Baird, *Polym. Eng. Sci.*, 36 (3), 378, (1996).
77 E.A. Sabol, *Master's Thesis*, Virginia Polytechnic Institute and State University, Blacksburg (VA) 1994.
78 E.A. Sabol, A.A. Handlos, and D.G. Baird, *Polym. Compos.*, 16 (4), 330 (1995).
79 A.M. Shibley, in *Handbook of Composites (Chap. 7)*, ed. G. Lubin, Van Nostrand Reinhold, New York 1982.
80 Schweizer and Winterman, in *Thermoplastic Polymer Additives: Theory and Practice*, ed. J.T. Lutz Jr., Marcel Dekker, New York 1989.
81 R.J. Crowson and M.J. Folkes, *Polym. Eng. Sci.*, 20 (14), 934 (1980).
82 L.A. Utracki and B. Fisa, *Polym. Comp.*, 3 (4), 193 (1982).
83 L.A. Utracki, *Rubber Chem. Tech.*, 57, 507 (1984).
84 B. Franzén, C. Klason, J. Kubát, and T. Kitano, *Composites*, 20 (1), 65 (1989).
85 S.H. Collins, *Plastics Compounding*, 5 (3), 113 (1982).
86 J.R. Gibson, P.S. Allan, and M.J. Bevis, *Compos. Manf.*, 1 (3), 183 (1990).
87 Anon., in *Modern Plastics Encyclopedia '92*, McGraw-Hill, New York (1992).
88 J. Barrett, *Eureka*, 12 (5), 41 (1992).
89 S. Kessler, in *Plastics Additives and Modifiers Handbook (Chap. 48)*, ed. J. Edenbaum, Van Nostrand Reinhold, New York 1992.
90 P.K. Mallick, *Fiber-Reinforced Composites*, Marcel Dekker, New York 1988.
91 W.R. Graner, in *Handbook of Composites*, ed. G. Lubin, Van Nostrand Reinhold, New York 1982.
92 S. Tomonoh, T. Tanaka, and Y. Omata, *37th International SAMPE Symposium (Materials Working for You in the 21st Century)*, 37, 1052 (1992).
93 C.L. Choy, W.P. Leung, K.W. Kowk, and F.P. Lau, *Polym. Compos.*, 13 (2), 69 (1992).
94 D.M. Bigg, *Polym. Compos.*, 6 (1), 20 (1985).
95 R.D. Kaverman, in *Plastics Engineering Handbook of the Society of the Plastics Industry, Inc. 5th ed. (Chap. 18)*, ed. M.L. Berins, Van Nostrand Reinhold, New York 1991.
96 L.M. Sherman, *Plastics Tech.*, 42 (9), 67 (1996).
97 H. Muramatsu and W.R. Krigbaum, *J. Polym. Sci.: Part B: Polym. Phys.*, 25, 2303 (1987).
98 J. Sarlin and P. Törmälä, *J. Appl. Polym. Sci.*, 50, 1225 (1993).
99 D. Acierno, F.R. La Mantia, G. Polizzotti, A. Ciferi, and B. Valenti, *Macromolecules*, 15, 1455 (1982).
100 Y. Ide and Z. Ophir, *Polym. Eng. Sci.*, 23, 261 (1983).
101 A.E. Zachariades and J.A. Logan, *Polym. Eng. Sci.*, 23, 797 (1983).
102 Y. Ide and T.S. Chung, *J. Macromol. Sci., Phys.*, B-23 (4-6), 497 (1984-85).

103 J.C. Jenkins and G.M. Jenkins, *J. of Mat. Sci.*, 22, 3784 (1987).
104 E. Suokas, J. Sarlin, and P. Törmälä, *Inst. Phys. Conf. Ser.*, 89 (3), 155 (1988).
105 K.J. Itoyama, *J. Polym. Sci., Polym. Phys. Ed.*, 26, 1845 (1988).
106 T.S. Chung, *J. Polym. Sci., Polym. Phys. Ed.*, 26, 1549 (1988).
107 A.T. DiBenedetto, L. Nicolais, E. Amendola, C. Carfagna, and M.R. Nobile, *Polym. Eng. Sci.*, 29 (3), 153 (1989).
108 K. Itoyama, *J. of Polym. Sci.: Part C: Polym. Lett.*, 27, 369 (1989).
109 J. Sarlin and P. Törmälä, *J. Appl. Polym. Sci.*, 40, 453 (1990).
110 H.N. Yoon, *Coll. Polym. Sci.*, 268, 230 (1990).
111 M.C. Muir and R.S. Porter, *Mol. Cryst. Liq. Cryst.*, 169, 91 (1989).
112 C. Robertson, *Master's Thesis*, Virginia Polytechnic Institute and State University, VA (1995).
113 J.M. Crosby, *33rd International SAMPE Symposium (Materials -- Pathway to the Future)*, 33, 1295 (1988).
114 R. Prescott, in *Modern Plastics Encyclopedia '92*, McGraw-Hill, New York (1992).
115 M.W.K. Rosenow, *40th International SAMPE Symposium (Materials Challenge: Diversification and the Future)*, 40 (2), 1534 (1995)
116 J.J. Pigliacampi, in *Modern Plastics Encyclopedia '92*, McGraw Hill, New York (1992).
117 L.K. English, *Materials Engineering*, 106 (7), 35 (1989).
118 C. Robertson, J.P. de Souza, and D.G. Baird, in *Liquid-Crystalline Polymer Systems: Technological Advances (Chap. 6) - ACS Symposium Series 632*, ed. A.I. Isayev, T. Kyu, and S.Z.D. Cheng, American Chemical Society, Washington (DC) 1996.
119 S.G. Advani, in *International Encyclopedia of Composites (Vol. 3)*, ed. S.M. Lee, VCH, New York (1990).
120 M.R. Kamal and A. Mutel, *J. Polym. Eng.*, 5 (4), 293 (1985).
121 A. Einstein, *Ann. Physik.*, 34, 591 (1911).
122 R.Z. Eisenschitz, *Z. Physik. Chem.*, A158, 85 (1971).
123 J.M. Burgers, *The Second Report on Viscosity and Plasticity*, Nordemann, New York (1938).
124 R. Schroder, *Rheol. Acta*, 20, 130 (1986).
125 T. Kitano and T. Kataoka, *Rheol. Acta*, 20, 390 (1981).
126 A.T. Mutel and M.R. Kamal, in *Two-phase Polymer Systems (Chap. 12)*, ed. L.A. Utracki, Hanser, New York (1991).
127 M.M. Cross, *J. Colloid Sci.*, 20, 417 (1965).
128 R.B. Bird, R.C. Armstrong, and O. Hassanger, *Dynamics of Polymeric Liquids (Vol. 1: Fluid Mechanics), 2nd ed.*, John Wiley and Sons, New York (1987).
129 M. Keentok, *Rheol. Acta*, 21, 325 (1982).
130 A.J. Poslinski, M.E. Ryan, R.K. Gupta, S.G. Seshadri, and F.J. Frechette, *J. Rheol.*, 32 (7), 703 (1988).
131 G.K. Batchelor, *J. Fluid Mech.*, 44 (3), 419 (1970).

132 G.K. Batchelor, *J. Fluid Mech.*, 46 (4), 813 (1971).
133 J. Mewis and A.B. Metzner, *J. Fluid Mech.*, 62 (3), 593 (1974).
134 T. Kitano, M. Funabashi, C. Klason, and J. Kubat, *Intl. Polym. Proc.*, 3, 67 (1988)
135 H.M. Laun, *Colloid Polym. Sci.*, 262, 257 (1984).
136 J.M. Dealy and K.F. Wissbrun, *Melt Rheology and its Role in Plastics Processing: Theory and Applications*, Van Nostrand Reinhold, New York (1990).
137 A.T. Mutel and M.R. Kamal, *SPE Tech. Pap.*, 32, 679 (1986).
138 N. Minagawa and J.L. White, *J. Appl. Polym. Sci.*, 20, 510 (1976).
139 H. Tanaka and J.L. White, *Polym. Eng. Sci.*, 20 (14), 949 (1980).
140 C.D. Han, C. Sandford, and H.J. Yoo, *Polym. Eng. Sci.*, 18 (11), 849 (1978).
141 C.D. Han, *J. Appl. Polym. Sci.*, 18, 821 (1974).
142 C.E. Chaffey, in *Proc. 2nd World Congress of Chem. Eng.*, Montreal (1981).
143 J.L White, L. Czarnecki, and H. Tanaka, *Rubb. Chem. Techn.*, 53, 823 (1980).
144 T. Kitano, T. Kataoka, and Y. Nagatsuka, *Rheol. Acta*, 23, 20 (1984).
145 Y. Chan, J.L. White, and Y. Oyanagi, *J. Rheol.*, 22 (5), 507 (1978).
146 L. Czarnecki and J.L. White, *J. Appl. Polym. Sci.*, 25, 1217 (1980).
147 S. Goto, H. Nagazono, and H. Kato, *Rheol. Acta*, 25, 246 (1986).
148 Y. Oyanagi and Y. Yamaguchi, *J. Soc. Rheol. Japan*, 3, 64 (1975).
149 J.D. Goddard, *J. Non-Newt. Fluid. Mech.*, 1, 1 (1976).
150 B. Yarlykov, *Intl. Polym. Sci. Tech.*, 4, T/7 (1977).
151 R.J. Crowson, M.J. Folkes, and P.F. Bright, *Polym. Eng. Sci.*, 20, 925 (1980).
152 R.J. Crowson and M.J. Folkes, *Polym. Eng. Sci.*, 20, 934 (1980).
153 S. Wu, *Polym. Eng. Sci.*, 19, 638 (1979).
154 W.W. Chan, J.M. Charrier, and P. Vadnas, *Polym. Compos.*, 4, 9 (1983).
155 C.D. Han, *Polym. Eng. Rev.*, 1, 363 (1981).
156 O.L. Forgacs and S.G. Mason, *J. Colloid Sci.*, 14, 457 (1959).
157 A. Salinas and J.F.T. Pittman, *Polym. Eng. Sci.*, 21 (1), 23 (1981).
158 R. Meyer, K.E. Almin, and B. Steenberg, *Brit. J. Appl. Phys.*, 17, 409 (1966).
159 J.M. Lunt and J.B. Shortall, *Plastics Rubber: Process*, 4 (3), 108 (1979).
160 J.M. Lunt and J.B. Shortall, *Plastics Rubber: Process*, 5 (2), 37 (1980).
161 R. von Turkovich and L. Erwin, *Polym. Eng. Sci.*, 23 (13), 743 (1983).
162 K. Stade, *Polym. Eng. Sci.*, 17 (1), 50 (1977).
163 B. Fisa, *Polym. Composites*, 6 (4), 232 (1985).
164 R.J. Nichols and M.A. Steller, *Plastics Compounding*, 9 (4), 14 (1986).
165 R.A. Schweizer, *Polym.-Plast. Technol. Eng.*, 18(1), 81 (1982).
166 R. Bailey and H. Kraft, *Intl. Polym. Proc.*, 2 (2), 94 (1987).
167 J.B. Shortall and D. Pennington, *Plastics Rubber Proc. Appl.*, 2 (1), 33 (1982).
168 W.-Y. Chiu and G.-D. Shyu, *J. Appl. Polym. Sci.*, 34, 1493 (1987).
169 J.E. Travis, D.A. Cianelli, and C.R. Gore, *Machine Design*, Feb. 12, 1987, pg 193.
170 J.E. Travis, D.A. Cianelli, and C.R. Gore, *RETEC '87*, 21-2, 336.

171 D.A. Cianelli, J.E. Travis, R.S. Bailey, in *43rd Ann. Conf., Composites Inst., The Society of the Plastics Industry*, Session 3-B, 1988.
172 D.A. Cianelli, J.E. Travis, R.S. Bailey, *Plastics Tech.*, 34 (4), 83 (1988).
173 J. Denault, T. Vu-Khanh, and B. Foster, *Polym. Comp.*, 10 (5), 313 (1989).
174 J. Denault, T. Vu-Khanh, D. Tailor, and A. Low, *SPE ANTEC '92 Tech. Papers*, 36, 788 (1992).
175 P.S. Allan and M.J. Bevis, *Plast. Rubber Proc. and Appl.*, 7, 3 (1987).
176 T.P. Skourlis, C. Chassapis, and S. Manoochehri, *J. of Thermoplastic Compos. Mat'ls*, 10 (5), 453 (1997).
177 G.B. Jeffery, *Proc. Roy. Soc.*, A102, 161 (1922).
178 M. Vincent and J.F. Agassant, in *Two-phase Polymer Systems (Chap. 11)*, ed. L.A. Utracki, Hanser, New York 1991.
179 H.L. Goldsmith and S.G. Mason, in *Rheology: Theory and Applications*, Vol. 4, ed. F.R. Eirich, Academic Press, New York (1967).
180 J.B. Harris and J.F.T. Pittman, *J. Colloid Interface Sci.*, 50, 280 (1975).
181 A.J. Godlman, R.G. Cox, and H. Brenner, *Chem. Eng. Sci.*, 22, 653 (1967).
182 M. Vincent, Y. Germain, J.F. Agassant, in *Progress and Trends in Rheology II*, ed. H. Giesekus and M.F. Hibberd, *Supp. Rheo. Acta*, 26, 144 (1988).
183 F.P. Folgar and C.L. Tucker III, *J. Reinf. Plast. Comp.*, 3, 98 (1984).
184 J.S. Cintra, Jr. and C.L. Tucker III, *J. Rheol.*, 39 (6), 1095 (1995).
185 G. Ausias, J.F. Agassant, and M. Vincent, *Intl. Polym. Proc.*, IX (1), 51 (1994).
186 S.M. Dinh and R.C. Armstrong, *J. Rheol.*, 28, 207 (1984).
187 C.G. Lipscomb, M.M. Denn, D.U. Hur, and D.V. Bogger, *J. Non-Newt. Fluid Mech.*, 26, 297 (1988).
188 E.S.G. Shaqfeh and G.H. Fredrickson, *Phys. Fluids A 2*, 7 (1990).
189 S.G. Advani and C.L. Tucker III, *J. Rheol.*, 34, 367 (1990).
190 A. Vaxman, M. Narkis, A. Siegman, and S. Kenig, *J. Mat. Sci., Lett.*, 7, 25 (1988).
191 S. Fakirov and C. Farikova, *Polym. Compos.*, 6, 41 (1985).
192 M. Sanou, B. Chung, and C. Cohen, *Polym. Eng. Sci.*, 25, 1008 (1985).
193 G. Fischer and P. Eyerer, *SPE Tech. Papers*, 32, 532 (1986).
194 M. Vincent and J.F. Agassant, *Polym. Compos.*, 7, 76 (1986).
195 S.G. Advani and C.L. Tucker III, *J. Rheol.*, 31, 751 (1987).
196 M.J. Folkes, D.A.M. Russell, *Polymer*, 21, 1252 (1980).
197 P.F. Bright, R.J. Crowson, and M.J. Folkes, *J. Mat. Sci.*, 13, 2497 (1978).
198 G. Akay, in *Interrelations Between Processing Structure and Properties of Polymeric Materials*, ed. J.C. Seferis and J.C. Theocaris, Elsevier Science Publishers, Amsterdam (1984).
199 S.H. Lim, T. Kikutani, J.L. White, and T. Kyu, *Adv. Polym. Tech.*, 8 (3), 325 (1988).
200 S.H. Lim and J.L. White, *J. Rheol.*, 34 (3), 343 (1990).
201 P.S. Allan and M.J. Bevis, *Plastics Rubber Proc. Appl.*, 7 (1), 3 (1987).

202 P.S. Allan and M.J. Bevis, in *Handbook of Polymer Fibre Composites*, ed. F.R. Jones, Longman Scientific and Technical, Essex 1994.
203 P.S. Allan, M.J. Bevis, *Composites Manufacturing*, 1 (2), 79 (1990).
204 J.R. Gibson, P.S. Allan, and M.J. Bevis, *Comp. Man.*, 1 (3), 183 (1990).
205 P.S. Allan and M.J. Bevis, *Plast. Rub. Comp. Proc. Appl.*, 16 (2), 133 (1991).
206 M.J. Bevis, *Makromol. Chem., Macromol. Symp.*, 22, 25 (1988).
207 L. Wang, P.S. Allan, and M.J. Bevis, *Plast. Rub. Comp. Proc. Appl.*, 23 (3), 139 (1995).
208 D.F. Hiscok and D.M. Bigg, *Polym. Compos.*, 10 (3), 145 (1989).
209 S.F. Xavier and A. Misra, *Polym. Compos.*, 6 (2), 93 (1985).
210 D.W. Clegg and A.A. Collyer, *Mechanical Properties of Reinforced Thermoplastics*, Elsevier Science Publications, New York 1986.
211 R.W. Richards and D. Sims, *Composites*, 2 (Dec.), 214 (1971).
212 J. Watkins, P. Gaa, and R. Swisher, *SPE ANTEC Tech. Papers*, 34, 528 (1988).
213 N. Sato, T. Kurauchi, S. Sato, and O. Kamigaio, *J. Composite Mat.*, 22 (9), 850 (1988).
214 D. McNally, *Polym.-Plast. Tech. Eng.*, 8 (2), 101 (1977).
215 B.F. Blumentritt, B.T. Vu, and S.L. Cooper, *Composites*, 6 (May), 105 (1975).
216 B.F. Blumentritt, B.T. Vu, and S.L. Cooper, *Polym. Eng. Sci.*, 14 (9), 633 (1974).
217 M.G. Bader and J.F. Collins, *Fibre Sci. and Tech.*, 18, 217 (1983).
218 M.W. Darlington, P.L. McGinley, and G.R. Smith, *J. Mat. Sci.*, 11, 877 (1976).
219 R.B. Pipes, R.L. McCullough, and D.G. Taggart, *Polym. Compos.*, 3 (1), 34 (1982).